Journal of Sound and Vibration 331 (2012) 5087–5106

Contents lists available at SciVerse ScienceDirect

Journal of Sound and Vibration

journal homepage: www.elsevier.com/locate/jsvi

The effect on bending waves by defects in pinned elastic plates

Michael J.A. Smith [a,*], Richard Porter [b], Timothy D. Williams [c]

[a] Department of Mathematics, University of Auckland, Private Bag 92019, Auckland, New Zealand
[b] School of Mathematics, University of Bristol, Bristol BS8 1TW, UK
[c] Nansen Environmental and Remote Sensing Center, Thormøhlens Gate 47, N-5006 Bergen, Norway

ARTICLE INFO

Article history:
Received 4 February 2012
Received in revised form
6 June 2012
Accepted 10 June 2012
Handling Editor: L.G. Tham
Available online 21 July 2012

ABSTRACT

This paper presents solutions to a number of problems posed for the out-of-plane displacement of infinite thin elastic plates that are rigidly pinned in periodic configurations, but that possess a finite number of 'defects'. We begin by considering a single one-dimensional periodic array of pins. We derive an analytic solution for the displacement produced by the forced oscillation of the central pin in the array, and this solution is shown to be closely connected to the problem of scattering of plane waves by an array when a finite number of pins are removed. Attention then focuses on doubly periodic rectangular arrays of pinned points possessing defects. Central to approaching such problems is an understanding of Bloch–Floquet waves in periodic arrays in the absence of defects and a simple method is described for computing the associated dispersion surfaces. The solutions to three problems are then sought: the trapping of localised waves by a finite number of missing pins; trapping of waves by entire rows of missing pins; and the wave radiation pattern due to the forcing of a single pin. All problems are treated analytically using bounded Green's functions for thin elastic plates, a discrete Fourier transform solution method and simple, explicit and rapidly convergent evaluations of the one- and two-dimensional lattice sums that arise.

1. Introduction

Thin elastic plates are used in many engineering applications and are often either bonded to a substructure along ribs or rigidly pinned by rivets. Determining the transmission properties due to defects in the vibrations along periodically ribbed elastic sheets and membranes was the subject of a series of significant papers published over a number of decades, e.g. [1–5]. In these investigations the elastic membrane, or thin elastic plate, is viewed in cross-section and bounded above by a two-dimensional acoustic or fluid medium. The interest in such problems lies in how sound waves couple with vibrational modes on a periodically supported elastic beam. The defects consisted of vibrating ribs and laterally displaced rib supports, the latter giving rise to localisation effects [6].

Evans and Porter [7,8], motivated in part by the work mentioned above, considered so-called Very Large Floating Structures in which they imagined a large two-dimensional thin elastic sheet secured to the sea bed by mooring lines that provided periodic point supports on the elastic sheet. In this situation, although the underlying three-dimensional incompressible fluid does not support body waves, coupling still exists between the fluid and elastic sheet. Their work highlighted the mathematical elegance of using point sources (or Green's functions) to represent the effect of point forces on an elastic sheet. In particular, whilst wave theories such as acoustics, electromagnetics and elasticity are governed by second-order partial differential

* Corresponding author. Tel.: +64 9 373 8768; fax: +64 9 373 7457.
E-mail address: m.smith@math.auckland.ac.nz (M.J.A. Smith).

0022-460X/$ - see front matter © 2012 Elsevier Ltd. All rights reserved.
http://dx.doi.org/10.1016/j.jsv.2012.06.013

equations, the Kirchhoff equation for a thin elastic plate is fourth-order in space. Consequently, point sources behave like $r^2 \log r$ as the distance r to the source is decreased rather than diverging like $\log r$ as in source solutions to second-order wave equations. This fact permits source functions to be used as physical representations of small clamped circular pins. We remark that isotropic point sources can be used as an approximate model for acoustic wave scatterers in the limit of small, widely spaced, soft-sound cylinders and long wavelengths, as discussed in Section 8.2.5 of Martin [9].

A variety of work on two-dimensional thin elastic sheets has followed, mainly choosing to ignore the complication of coupling to an external fluid or acoustic medium (such problems have been examined by [10–12] for both arrays of pins and point masses). For example, Movchan et al. [13] computed the band-gap structure for a doubly periodic arrangement of holes of finite radius with either clamped or free edges. The dispersion relation for Bloch–Floquet waves through a periodically pinned sheet was obtained analytically by taking the limit of a clamped hole radius tending to zero. This particular problem, whose solution also appears in Evans and Porter [8], is revisited in Section 3 of the current paper where a simpler approach to computing the band-gap structure is described. Other recent related works on pinned elastic plates include [14–17].

The focus of the present paper is to examine the effect of introducing 'defects' into both one- and two-dimensional infinite periodic arrays of rigidly pinned points in a thin elastic plate. In this paper a defect will mean either removing one or more pins from the array, or replacing a rigid pin by one which is forced to oscillate periodically in time at a prescribed amplitude. The mathematical difficulty in solving defect problems of this type arises as the geometry is no longer periodic.

Defects in one-dimensional periodic arrays have been considered in the setting of the two-dimensional Helmholtz equation for a linear array of acoustically-hard or soft cylinders by Thompson and Linton [18]. There the solution is approached using the so-called 'Modified Array Scanning Method'. Its use of transform methods and excitation of waves by point sources to represent the defects bears similarities to the approach used in the present paper. However, our methods proceed more directly and transparently, evidently due to the simplicity afforded by using single point sources to represent pins. Earlier, Thompson and Linton [19] had used the array scanning method to consider the excitation of an acoustic wave field by a line source in the presence of a periodic array of cylinders.

Defects in doubly periodic arrays are of current interest in several research fields including elastodynamics [20], phononic crystals [21] and photonic crystals [22–26]. Techniques for determining defect modes range from the method of fictitious sources, to supercell methods and multipole methods. Attention has also been focused on understanding the effects of defects in more complicated photonic structures such as woodpiles [27].

Recently, [28] published related work considering the problems of single point and line defects which independently reproduces some of the results here. They also considered forcing and defects in doubly periodic arrays of point masses, as well as rigid pins. The interaction theory developed herein is able to accommodate multiple defects, as well as single defects, for doubly periodic arrays of rigid pins.

Bloch–Floquet problems occur frequently in many application areas of the physical sciences and central to the understanding of defects in doubly periodic arrays is the consideration of the associated homogeneous problem without defects. Often they are related to the solution of the wave (or Helmholtz's) equation which requires the evaluation of lattice sums which in their most basic form are poorly convergent. Hence acceleration of lattice sums for computational purposes is crucial. As a result, efficient methods for the evaluation of convergent lattice sums (using Graf's addition theorem and integral techniques) for Helmholtz's equation in a doubly periodic domain continue to be developed, e.g. [29–31]. Linton [32] provides an exhaustive survey of the most commonly used techniques.

In contrast to those methods cited above for Helmholtz's equation, here we are able to derive convergent, readily computable lattice sums for problems posed using the thin elastic plate equation by applying standard methods, without the need to accelerate convergence characteristics. This is evidently a consequence of the low order of the condition applied at pinned points (zero) compared to the order of the governing equation (four). In particular, this means that the Green's function that produces the point sources used to represent the pinned points is bounded everywhere.

Our general method of solution is applied first in Section 2 to one-dimensional arrays. The roots of this method can be traced to Crighton [2] and are based on Fourier transforming the infinite systems of equations that arise from the application of pin conditions. Two distinct problems naturally arise: the wave radiation pattern due to the time-harmonic forcing of the central pin and the scattering of plane waves by a number of missing pins in an array.

Solution methods for linear periodic arrays are then extended to more complicated and arguably more interesting problems involving doubly periodic arrays of pins, and here we investigate the possible localised modes that are supported by defects. In total, three problems are considered here: the effect of removing one or more pins from the plate; the wave radiation pattern due to the forced motion of a single pin; and the effect of removing entire rows of pins. These are presented in Section 3, and in Section 4, and a selection of results are presented from each of the problems considered in the paper. The work is summarised in Section 5 where an indication is given as to how these methods may be extended to other related and physically interesting problems.

2. Defects in a single periodic array of pinned points

An infinite thin elastic plate occupies the $(\overline{x},\overline{y})$ plane having an out-of-plane displacement $\overline{u}(\overline{x},\overline{y})$, and is assumed to be pinned rigidly along the line $\overline{y}=0$ at $\overline{x}=m\overline{a}$ for $m \in \mathbb{Z}\backslash\mathcal{M}$ where $\mathcal{M}$ is a finite set which represents points in an otherwise periodic array which are not rigidly pinned (i.e. defects). In the simplest case $\mathcal{M}=\{0\}$ represents a single defect at the origin. The period of the array is represented by $\overline{a}$, and we consider two problems in this section. In the first, $\mathcal{M}=\{0\}$ and in

its place, the point (0,0) is excited by a forcing of amplitude C at angular frequency ω. (This problem shall be referred to as the forced pin problem.) In the second problem, a periodic array with defects is excited by an incident plane wave of fixed amplitude and angular frequency ω from infinity, propagating at an angle θ_0 with the negative $\overline{y}$-axis.

In both cases, the governing equation for a thin elastic plate is given by

$$(\overline{\Delta}^2-k^4)\overline{u}(\overline{x},\overline{y})=0, \tag{1}$$

after removing a time dependence of $e^{-i\omega t}$. Here $\overline{\Delta}$ is the two-dimensional Laplacian, $k^4=m\omega^2/D$, $m=\rho h$ is the mass per unit area in terms of the plate thickness h and density ρ, and $D=(1/12)Eh^3/(1-\nu^2)$ is the flexural rigidity defined in terms of Young's modulus E and Poisson's ratio ν. The conditions at the fixed pins are

$$\overline{u}(m\overline{a},0)=0, \quad m\in\mathbb{Z}\backslash\mathcal{M}. \tag{2}$$

Nondimensionalising lengths with respect to k via $x=k\overline{x}$, $y=k\overline{y}$ and $a=k\overline{a}$ with $u(x,y)=k\overline{u}(\overline{x},\overline{y})$ converts (1) and (2) into

$$(\Delta^2-1)u(x,y)=0, \tag{3}$$

and

$$u(ma,0)=0, \quad m\in\mathbb{Z}\backslash\mathcal{M}. \tag{4}$$

Thus, the problem depends only on the single dimensionless parameter a.

We first consider the problem of pin forcing at the centre of the one-dimensional periodic array. This solution is then used to construct the solution to the scattering of plane waves by a defective array in the following subsection.

2.1. Forcing of the central pin

Here we consider the problem of forcing a single pin with unit amplitude in a periodic linear array of pinned points in the absence of an incident wave field. We use the superscript (f) throughout to distinguish this problem from later problems, and introduce the notation $u_m^{(f)}=u^{(f)}(ma,0)$, $m\in\mathbb{Z}$, to represent the displacement at the point $x=ma$ in the array. For this problem $\mathcal{M}=\{0\}$ and the pinned conditions $u_m^{(f)}=0$ are set for $m\notin\mathcal{M}$ whilst at the origin $u_0^{(f)}=1$ is imposed. The total displacement of the plate can be written as

$$u^{(f)}(x,y)=\sum_{n=-\infty}^{\infty}a_n^{(f)}g(x-na,y), \tag{5}$$

where $g(x,y)$ represents a Green's function for a source placed at the origin of a thin plate satisfying

$$(\Delta^2-1)g(x,y)=\delta(x)\delta(y), \tag{6}$$

and is given explicitly by

$$g(x,y)=\tfrac{i}{8}(H_0(r)-H_0(ir)), \tag{7}$$

where $H_0\equiv H_0^{(1)}$ represents a Hankel function of the first kind and $r^2=x^2+y^2$. Note that at the origin the Green's function is bounded as $g(0,0)=i/8$.

In (5), the coefficients $a_n^{(f)}$ are to be determined. Enforcing the boundary conditions at each point in the array on (5) gives

$$u_m^{(f)}=\sum_{n=-\infty}^{\infty}a_n^{(f)}g((m-n)a,0)=\delta_{m0}, \tag{8}$$

for all m, where δ_{mn} represents the Kronecker delta function. Accordingly, multiplying through by $e^{-im\theta}$ and summing over all m results in

$$1=\sum_{m=-\infty}^{\infty}\sum_{n=-\infty}^{\infty}a_n^{(f)}g((m-n)a,0)e^{-im\theta}, \tag{9}$$

where θ refers to the standard angular polar coordinate.

We now define the following finite Fourier transforms (Fourier series) with

$$A^{(f)}(\theta)=\sum_{n=-\infty}^{\infty}a_n^{(f)}e^{-in\theta}, \quad a_n^{(f)}=\frac{1}{2\pi}\int_{-\pi}^{\pi}A^{(f)}(\theta)e^{in\theta}\,d\theta, \tag{10a}$$

$$G_0(\theta;a)=\sum_{n=-\infty}^{\infty}g(na,0)e^{-in\theta}, \quad g(na,0)=\frac{1}{2\pi}\int_{-\pi}^{\pi}G_0(\theta;a)e^{in\theta}\,d\theta. \tag{10b}$$

The series in (10b) has been computed in Evans and Porter [7] and it helps to outline this process here. Thus, the integral representations of the Hankel functions allow us to write the Green's function as

$$g(x,y)=\frac{1}{8\pi}\int_{-\infty}^{\infty}\mathcal{G}(t,y)e^{ixt}\,dt, \quad \mathcal{G}(t,y)=\frac{e^{-\lambda(t)|y|}}{\lambda(t)}-\frac{e^{-\gamma(t)|y|}}{\gamma(t)}, \tag{11}$$

where

$$\lambda(t)=\begin{cases}(t^2-1)^{1/2}, & t\geq 1,\\ -\mathrm{i}(1-t^2)^{1/2}, & -1<t<1,\\ (t^2-1)^{1/2}, & t\leq -1,\end{cases}\quad\text{and}\quad \gamma(t)=(1+t^2)^{1/2}. \tag{12}$$

Note that $\lambda(t)$ is decomposed in this manner to emphasise that the integrand $\mathcal{G}$ is analytic on an appropriately cut Riemann surface. Alternative integral representations involving paths of integration in the complex field can be found in Watson [33]. Applying the Poisson summation formula

$$2\pi\sum_{n=-\infty}^{\infty} f(2n\pi)=\sum_{n=-\infty}^{\infty}\int_{-\infty}^{\infty}\mathrm{e}^{\pm \mathrm{i}nu}f(u)\,\mathrm{d}u, \tag{13}$$

to expression (11) at the points $(x,y)=(na,0)$ and comparing with (10b) readily admits the convergent series

$$G_0(\theta;a)=\frac{1}{4a}\sum_{n=-\infty}^{\infty}\mathcal{G}(t_n,0), \tag{14}$$

where $t_n=(\theta+2n\pi)/a$. It can be shown that the summand $\mathcal{G}(t_n,0)$ has a leading order asymptotic behaviour of $a^3/(2\pi|n|)^3$ as $|n|\to\infty$, so convergence can be accelerated by writing

$$G_0(\theta;a)=\frac{1}{4a}\left(\mathcal{G}(t_0,0)+\frac{2a^3}{(2\pi)^3}\zeta(3)\right)+\frac{1}{4a}\sum_{n=1}^{\infty}\left(\mathcal{G}(t_n,0)+\mathcal{G}(t_{-n},0)-\frac{2a^3}{(2n\pi)^3}\right), \tag{15}$$

where ζ denotes the Riemann zeta function. This forces (15) to converge like $O(|n|^{-5})$. It can also be seen that G_0 is both symmetric and periodic

$$G_0(-\theta;a)=G_0(\theta;a),\quad G_0(\theta+2m\pi;a)=G_0(\theta;a)\ \text{ for } m\in\mathbb{Z}. \tag{16}$$

The definitions above allow expression (9) for the forcing of a single pin to be written in the form

$$1=A^{(f)}(\theta)G_0(\theta;a), \tag{17}$$

after using the convolution result for Fourier series. Rearranging (17) for $A^{(f)}(\theta)$ and inverting from (10a) admits

$$a_n^{(f)}=\frac{1}{2\pi}\int_{-\pi}^{\pi}\frac{\mathrm{e}^{\mathrm{i}n\theta}}{G_0(\theta;a)}\,\mathrm{d}\theta, \tag{18}$$

which is the final form of the scattering coefficient.

It is proved in Evans and Porter [7] that $G_0(\theta;a)$ does not vanish, and this postpones the complications associated with singularities in integrals that we encounter in later parts of the paper.

As a corollary to the above solution, we can see from (8) that

$$\begin{aligned}\sum_{n=-\infty}^{\infty}a_{n-r}^{(f)}g((m-n)a,0)&=\sum_{n'=-\infty}^{\infty}a_{n'}^{(f)}g((m-r-n')a,0)\\ &=\delta_{m-r,0}=\delta_{mr}.\end{aligned} \tag{19}$$

Therefore, once the coefficients $a_n^{(f)}$ have been determined from the problem of forcing a pin at the origin, the coefficients needed for forcing the rth pin are just $a_{n-r}^{(f)}$.

To determine the far-field behaviour of the displacement, we can decompose the integral representation of the Green's function (11) into integrands that either oscillate or decay exponentially with y:

$$g(x,y)=\frac{\mathrm{i}}{8\pi}\int_{-1}^{1}\frac{\mathrm{e}^{\mathrm{i}xt+\mathrm{i}(1-t^2)^{1/2}|y|}}{(1-t^2)^{1/2}}\,\mathrm{d}t+\frac{1}{8\pi}\int_{-\infty}^{\infty}\widehat{\mathcal{G}}(t,y)\mathrm{e}^{\mathrm{i}xt}\,\mathrm{d}t, \tag{20a}$$

where

$$\widehat{\mathcal{G}}(t,y)=\begin{cases}-\dfrac{\mathrm{e}^{-\gamma(t)|y|}}{\gamma(t)} & \text{if } |t|<1,\\ \dfrac{\mathrm{e}^{-(t^2-1)^{1/2}|y|}}{(t^2-1)^{1/2}}-\dfrac{\mathrm{e}^{-\gamma(t)|y|}}{\gamma(t)} & \text{if } |t|\geq 1.\end{cases} \tag{20b}$$

Substituting (20a) into (5), we note that the dominant contribution to the far-field displacement will come from the first integral in (20a) as it decays like $\rho^{-1/2}$ (where $x+\mathrm{i}y=\rho\mathrm{e}^{\mathrm{i}\chi}$ in polar coordinates) due to its phase becoming stationary, while the second integral involving $\hat{\mathcal{G}}$ is $O(\rho^{-3/2})$. Therefore, after using the Fourier series definition (10a), we find that

$$u^{(f)}=\frac{1}{8\pi}\int_{-\infty}^{\infty}A^{(f)}(at)\mathcal{G}(t,y)\mathrm{e}^{\mathrm{i}tx}\,\mathrm{d}t\sim\frac{\mathrm{i}}{8\pi}\int_{-1}^{1}\frac{A^{(f)}(at)}{(1-t^2)^{1/2}}\mathrm{e}^{\mathrm{i}xt+\mathrm{i}(1-t^2)^{1/2}|y|}\,\mathrm{d}t,\quad\text{as } \rho\to\infty. \tag{21}$$

Now, due to the symmetry of our problem, we can restrict ourselves to the half-plane $y>0$, and only consider $0<\chi<\pi$. Then (21) can be rewritten as

$$u^{(f)} \sim \frac{\mathrm{i}}{8\pi}\int_0^{\pi} A^{(f)}(a\cos\tau)\mathrm{e}^{\mathrm{i}\rho\cos(\tau-\chi)}\,\mathrm{d}\tau, \quad \text{as } \rho\to\infty. \tag{22}$$

Applying the method of stationary phase, one can directly obtain the result

$$u^{(f)} \sim \left(\frac{2}{\pi\rho}\right)^{1/2}\mathrm{e}^{\mathrm{i}(\rho-\pi/4)}A_\infty^{(f)}(\chi), \quad \text{as } \rho\to\infty, \tag{23a}$$

where the diffraction amplitude is

$$A_\infty^{(f)}(\chi) = \frac{\mathrm{i}}{8}A^{(f)}(a\cos\chi). \tag{23b}$$

This result can also be obtained by substituting the asymptotic form of the Green's function for large arguments from (7) into (5), and can also be continued into the half-plane $-\pi<\chi<0$ by reflection in the array.

2.2. Scattering of plane waves by defects in a 1D periodic array

We now move on to considering plane wave scattering by a linear periodic array of pinned points containing a finite number of missing pins, encoded in the set $\mathcal{M}$. The superscript (s) is used to denote quantities associated with this scattering problem. Here, we let $u_m^{(s)} = u^{(s)}(ma,0)$ for all m and so $u_m^{(s)}=0$ for $m\in\mathbb{Z}\backslash\mathcal{M}$. The total displacement is written as

$$u^{(s)}(x,y) = u^{(i)}(x,y) + \sum_{n=-\infty}^{\infty} a_n^{(s)} g(x-na,y), \tag{24}$$

where the prescribed incident wave plate displacement is given by

$$u^{(i)}(x,y) = \mathrm{e}^{\mathrm{i}\alpha_0 x+\lambda(\alpha_0)y}, \tag{25}$$

with $\alpha_0=\sin\theta_0$ and $\lambda(\alpha_0)=-\mathrm{i}\cos\theta_0$ as defined in (12).

In expression (24), the coefficients $a_n^{(s)}$, $n\notin\mathcal{M}$ are to be determined, whilst we set $a_n^{(s)}=0$ for $n\in\mathcal{M}$ since there is no contribution to the scattered field from pins that are removed from the array. Enforcing the pinned conditions on the general solution (24) gives

$$0 = u^{(i)}(ma,0) + \sum_{n=-\infty}^{\infty} a_n^{(s)} g((m-n)a,0), \quad m\notin\mathcal{M}. \tag{26}$$

For $m\in\mathcal{M}$, the left hand side of the above expression is replaced with the unknown displacement at each of the removed pins,

$$u_m^{(s)} = u^{(i)}(ma,0) + \sum_{n=-\infty}^{\infty} a_n^{(s)} g((m-n)a,0), \quad m\in\mathcal{M}. \tag{27}$$

Eqs. (26) and (27) can consequently be combined and written in the suggestive form

$$\sum_{r\in\mathcal{M}} u_r^{(s)}\delta_{mr} = u^{(i)}(ma,0) + \sum_{n=-\infty}^{\infty} a_n^{(s)} g((m-n)a,0), \quad m\in\mathbb{Z}. \tag{28}$$

The structure of (28) allows a solution to be written as a superposition of the separate effects of incident wave scattering by an unbroken periodic array and forcing of strength $u_r^{(s)}$ at each of locations $r\in\mathcal{M}$ in the absence of an incident wave. In other words,

$$a_n^{(s)} = a_n^{(u)} + \sum_{r\in\mathcal{M}} u_r^{(s)} a_{n-r}^{(f)}, \tag{29}$$

which follows from the use of the forcing solution (19). Here the coefficients $a_n^{(f)}$ have been previously determined by (18), whilst $a_n^{(u)}$ is the solution of

$$-u^{(i)}(ma,0) \equiv -\mathrm{e}^{\mathrm{i}m\alpha_0 a} = \sum_{n=-\infty}^{\infty} a_n^{(u)} g((m-n)a,0), \quad m\in\mathbb{Z}, \tag{30}$$

which is the equation for plane wave scattering by an uninterrupted grating. The periodicity of the left-hand side of (30) implies a periodicity of the solution, i.e. $a_n^{(u)} = a_0^{(u)}\mathrm{e}^{\mathrm{i}n\alpha_0 a}$. Substituting this in (30) gives

$$-1 = a_0^{(u)}\sum_{n=-\infty}^{\infty} g(-na,0)\mathrm{e}^{\mathrm{i}n\alpha_0 a} = a_0^{(u)}G_0(-\alpha_0 a;a) = a_0^{(u)}G_0(\alpha_0 a;a), \tag{31}$$

after using (10b) and (16), and so the final form of (29) is

$$a_n^{(s)} = -\frac{e^{in\alpha_0 a}}{G_0(\alpha_0 a; a)} + \sum_{r\in\mathcal{M}} u_r^{(s)} a_{n-r}^{(f)}. \tag{32}$$

The remaining unknowns, $u_r^{(s)}$ for $r \in \mathcal{M}$, are determined by imposing the remaining condition $a_n^{(s)} = 0$ for $n \in \mathcal{M}$ in (32) resulting in the linear system

$$\frac{e^{in\alpha_0 a}}{G_0(\alpha_0 a; a)} = \sum_{r\in\mathcal{M}} u_r^{(s)} a_{n-r}^{(f)}, \quad n \in \mathcal{M}. \tag{33}$$

When a single pin at the origin is missing, that is $\mathcal{M} = \{0\}$, the solution of (32) and (33) is given explicitly by

$$a_n^{(s)} = \frac{1}{G_0(\alpha_0 a; a)}\left(-e^{in\alpha_0 a} + \frac{a_n^{(f)}}{a_0^{(f)}}\right). \tag{34}$$

In the scattering problem, there are two components to the far-field: plane waves which are reflected and transmitted by an uninterrupted periodic grating as well as circular waves emanating from the defects. In the case of a single missing pin at the origin, these circular waves are easily identified from the second term in (34) to be related to those for the forcing problem, so that the diffraction coefficient for the circular wave component of the scattered field is simply

$$A_\infty^{(s)}(\chi) = \frac{A_\infty^{(f)}(\chi)}{a_0^{(f)} G_0(\alpha_0 a; a)}, \tag{35}$$

with $A_\infty^{(f)}$ defined by (23b). More generally, for multiple missing pins, the contribution from the sum in (32) to far-field circular waves results in a diffraction coefficient given by

$$A_\infty^{(s)}(\chi) = A_\infty^{(f)}(\chi) \sum_{m\in\mathcal{M}} u_m^{(s)} e^{-ima\cos\chi}. \tag{36}$$

The first term in the right-hand side of either (32) or (34) accounts for the diffracted wave field from an unbroken periodic array and its contribution to the total displacement may be written as

$$u^{(u)}(x,y) = -\frac{1}{G_0(\alpha_0 a; a)} \sum_{n=-\infty}^{\infty} e^{in\alpha_0 a} g(x-na, y). \tag{37}$$

Using the integral representation (11) in the above and invoking Poisson's summation formula gives

$$u^{(u)}(x,y) = \frac{-1}{4aG_0(\alpha_0 a; a)} \sum_{n=-\infty}^{\infty} e^{i\alpha_n x}\left(\frac{e^{-\lambda(\alpha_n)|y|}}{\lambda(\alpha_n)} - \frac{e^{-\gamma(\alpha_n)|y|}}{\gamma(\alpha_n)}\right), \tag{38}$$

where

$$\alpha_n = \alpha_0 + 2n\pi/a. \tag{39}$$

We can define scattering angles θ_n, defined by $\alpha_n = \sin\theta_n$, which extend the definition of $\alpha_0 = \sin\theta_0$ introduced for the incident wave. Then, providing $|\alpha_n| < 1$, θ_n are real angles corresponding to propagating waves and we say that $n \in \mathcal{N}$ (note that $\mathcal{N}$ is nonempty as it always contains the zero element.) For such values of n, $\lambda(\alpha_n) = -i\cos\theta_n$, allowing (38) to be written as

$$u^{(u)}(x,y) \sim \frac{-1}{4aG_0(\alpha_0 a; a)} \sum_{n\in\mathcal{N}} \frac{e^{ix\sin\theta_n} e^{i|y|\cos\theta_n}}{(-i\cos\theta_n)}, \tag{40}$$

as $|y| \to \pm\infty$. For $y > 0$, (40) represents reflected plane waves propagating away from the array (located at $y=0$) at scattering angles θ_n with amplitudes $R_n = -i/(4aG_0(\alpha_0 a; a)\cos\theta_n)$ whilst for $y < 0$, the superposition of the incident wave field implies transmitted wave amplitudes of $T_n = \delta_{n0} + R_n$. These are well-known effects in diffraction grating theory [7].

3. Defects in a doubly periodic array of pinned points

We now move on to consider problems involving doubly periodic arrays of pinned points. Specifically, we choose to pin an infinite elastic plate at the points $(x,y)=(na,mb)$ for $(n,m) \in \mathbb{Z}_2\backslash\mathcal{M}$, where a and b denote the periodicity of the rectangular lattice in the two perpendicular directions on the plate. The set $\mathcal{M}$ represents lattice indices where defects occur, i.e. where pins are missing. In the simplest case of a single defect at the origin, $\mathcal{M} = \{(0,0)\}$. There are two problems we can consider here. The first problem is one in which the origin is forced to oscillate with a set frequency and unit amplitude. The interest here lies in how the radiated wave energy may escape through the lattice to infinity as a function of angular frequency, ω. The second is the possibility of locating trapped modes in the vicinity of the defect(s) in the lattice. These are localised wave motions which oscillate indefinitely and do not radiate energy away to infinity within the otherwise periodic lattice of pinned points.

As we shall show, both problems require information about Bloch–Floquet waves in an infinite doubly periodic lattice without defects, which will appear as a byproduct of our analysis.

3.1. Forcing of the central pin

Let us again first consider the forcing problem, as the defect problem can be written as a superposition of solutions to the forcing problem over the set of defects (as shown in Section 2). A general solution is written as

$$u^{(f)}(x,y)=\sum_{n=-\infty}^{\infty}\sum_{m=-\infty}^{\infty}a_{nm}^{(f)}g(x-na,y-mb), \tag{41}$$

where we impose the pinned conditions $u_{nm}^{(f)}\equiv u^{(f)}(na,mb)=0$, $(n,m)\notin\mathcal{M}$, where $\mathcal{M}=\{(0,0)\}$. At the origin we set $u_{00}^{(f)}=1$ to represent the forcing. Applying these conditions to (41) gives

$$\delta_{p0}\delta_{q0}=\sum_{n=-\infty}^{\infty}\sum_{m=-\infty}^{\infty}a_{nm}^{(f)}g((p-n)a,(q-m)b), \tag{42}$$

for all $p,q\in\mathbb{Z}$. Multiplying this through by $\mathrm{e}^{-\mathrm{i}p\theta}\mathrm{e}^{-\mathrm{i}q\phi}$ and summing over all p and q results in

$$1=\sum_{p=-\infty}^{\infty}\sum_{q=-\infty}^{\infty}\sum_{n=-\infty}^{\infty}\sum_{m=-\infty}^{\infty}a_{nm}^{(f)}g((p-n)a,(q-m)b)\mathrm{e}^{-\mathrm{i}p\theta}\mathrm{e}^{-\mathrm{i}q\phi}. \tag{43}$$

Using the convolution result for Fourier series and rearranging, this can be expressed as

$$1=A^{(f)}(\theta,\phi)G(\theta,\phi;a,b), \tag{44}$$

where

$$A^{(f)}(\theta,\phi)=\sum_{n=-\infty}^{\infty}\sum_{m=-\infty}^{\infty}a_{nm}^{(f)}\mathrm{e}^{-\mathrm{i}n\theta}\mathrm{e}^{-\mathrm{i}m\phi}, \tag{45}$$

and

$$G(\theta,\phi;a,b)=\sum_{n=-\infty}^{\infty}\sum_{m=-\infty}^{\infty}g(na,mb)\mathrm{e}^{-\mathrm{i}n\theta}\mathrm{e}^{-\mathrm{i}m\phi}, \tag{46}$$

whilst the inversion formula associated with (45) is

$$a_{nm}^{(f)}=\frac{1}{4\pi^2}\int_{-\pi}^{\pi}\int_{-\pi}^{\pi}A^{(f)}(\theta,\phi)\mathrm{e}^{\mathrm{i}n\theta}\mathrm{e}^{\mathrm{i}m\phi}\,\mathrm{d}\theta\,\mathrm{d}\phi. \tag{47}$$

Equation (46) defining $G(\theta,\phi;a,b)$ is a double lattice sum and in the present form is not suitable for computation as the series is very slowly convergent. We follow the procedure already used for a single periodic array to convert (46) into a more convergent series. Thus, we use the integral representation (11) in (46) to give

$$G(\theta,\phi;a,b)=\frac{1}{8\pi}\sum_{m=-\infty}^{\infty}\sum_{n=-\infty}^{\infty}\int_{-\infty}^{\infty}\mathcal{G}(t,mb)\mathrm{e}^{\mathrm{i}n(at-\theta)-\mathrm{i}m\phi}\,\mathrm{d}t. \tag{48}$$

Using Poisson's summation formula for the n summation gives

$$G(\theta,\phi;a,b)=\frac{1}{4a}\sum_{m=-\infty}^{\infty}\sum_{n=-\infty}^{\infty}\left(\frac{\mathrm{e}^{-\lambda(t_n)|m|b}}{\lambda(t_n)}-\frac{\mathrm{e}^{-\gamma(t_n)|m|b}}{\gamma(t_n)}\right)\mathrm{e}^{-\mathrm{i}m\phi}, \tag{49}$$

where $t_n=(\theta+2n\pi)/a$ again. Then, reversing the order of summation in (49) and summing the resulting geometric series for m gives, after some routine algebra,

$$G(\theta,\phi;a,b)=\frac{1}{4a}\sum_{n=-\infty}^{\infty}\left(\frac{1}{\lambda(t_n)}\frac{\sinh(\lambda(t_n)b)}{\cosh(\lambda(t_n)b)-\cos\phi}-\frac{1}{\gamma(t_n)}\frac{\sinh(\gamma(t_n)b)}{\cosh(\gamma(t_n)b)-\cos\phi}\right), \tag{50}$$

which is now absolutely convergent. We observe that

$$G(\theta+2p\pi,\phi+2q\pi;a,b)=G(\theta,\phi;a,b),\quad \text{for } p,q\in\mathbb{Z}, \tag{51a}$$

$$G(\theta,\phi;a,b)=G(\theta,-\phi;a,b)=G(-\theta,\pm\phi;a,b), \tag{51b}$$

and also that G is real-valued. Returning to (44), and inverting the transform using (47) gives

$$a_{nm}^{(f)}=\frac{1}{4\pi^2}\int_{-\pi}^{\pi}\int_{-\pi}^{\pi}\frac{\mathrm{e}^{\mathrm{i}n\theta}\mathrm{e}^{\mathrm{i}m\phi}}{G(\theta,\phi;a,b)}\,\mathrm{d}\theta\,\mathrm{d}\phi. \tag{52}$$

In contrast to Section 2, in which coefficients were defined in terms of a single integral with a denominator G_0 which is strictly positive, in (52) there is the possibility that G will vanish along curves in the two-dimensional domain of integration.

We therefore consider the implication of vanishing G. Problems of this type have a long history and we direct interested readers to Martin [34] for a survey on the solution methods of Lipshitz and Koster (in the setting of the reduced wave equation), as well as section 4.9 of Lighthill [35]. The work of these authors is all pertinent to the calculations we have performed here and highlight the different approaches that can be used. Applying any of these methods to our integral (51) gives the same result we have derived here.

A reworking of (43) and (44) in the case of a doubly periodic array without any defects results in homogeneous versions of those equations and hence nontrivial solutions are found when

$$G(\theta,\phi;a,b)=0. \tag{53}$$

The resulting solutions have the quasi-periodicity property in that the expansion coefficients $a_{mn}^{(b)}$ used in place of $a_{mn}^{(f)}$ in (41), satisfy the relation

$$a_{mn}^{(b)}=a_{00}^{(b)}\mathrm{e}^{\mathrm{i}n\theta}\mathrm{e}^{\mathrm{i}m\phi}=a_{00}^{(b)}\mathrm{e}^{\mathrm{i}\mathbf{r}_{nm}\cdot\boldsymbol{\alpha}},$$

where $\mathbf{r}_{nm}\equiv(na,mb)$ are position vectors of pins in the array, $\boldsymbol{\alpha}=(\alpha,\beta)$ is the Bloch wave vector and $\theta\equiv\alpha a$, $\phi\equiv\beta b$. Such solutions represent Bloch–Floquet waves (hence the superscript (b)). It helps to make full use of this change of coordinates to define

$$\tilde{G}(\boldsymbol{\alpha};a,b)=G(\theta,\phi;a,b), \tag{54}$$

defined on $-\pi/a\le\alpha\le\pi/a$ and $-\pi/b\le\beta\le\pi/b$, the fundamental cell of the reciprocal lattice. Solutions of (53) form propagation surfaces in (α,β,a)-space which depend on the lattice aspect ratio b/a. Assuming the aspect ratio b/a and dimensionless frequency a to be fixed, $\tilde{G}$ vanishes along the curves of constant frequency on the propagation surfaces satisfying $\tilde{G}=0$. If $\tilde{G}\neq0$ throughout the fundamental cell of the reciprocal lattice then the frequency a is said to lie in a stop-band; wave propagation is impossible in all directions. Otherwise the frequency is said to lie in a pass band and waves can propagate throughout the infinite array. The permissible directions of wave propagation are not defined by the direction of the Bloch wave vector (α,β) along the curves of constant frequency, but in the direction of $\nabla\tilde{G}\equiv(\tilde{G}_\alpha,\tilde{G}_\beta)$ evaluated along those curves. This is because energy propagates in the direction of the group velocity vector, and not in the direction of the phase vector [36].

To distinguish between $\pm\nabla\tilde{G}$, which are both given by lines normal to the constant-frequency contours of the band surfaces, we can follow Lighthill [35]. From a causality argument (see also [37,38] for a good discussion of radiation conditions), he required that energy could only radiate in a direction $\mathbf{n}$ if $\mathbf{c}_g\cdot\mathbf{n}>0$, where the group velocity $\mathbf{c}_g$ is defined by $d\omega=\mathbf{c}_g\cdot\mathrm{d}\overline{\boldsymbol{\alpha}}$, where $\overline{\boldsymbol{\alpha}}$ is the dimensional wave vector. From this definition, the radiation condition is equivalent to requiring $\mathrm{d}\omega>0$ when we move in the direction $\mathbf{n}$ along the dispersion surface.

In our case, $a=k\overline{a}\propto\omega^{1/2}$ acts as a proxy for the frequency ω so we apply the condition that energy can propagate in a direction $\mathbf{n}$ if $\mathrm{d}a>0$ when we travel along the band surface. If we also let $\tilde{\mathbf{c}}_g=-(\partial_a\tilde{G})^{-1}\nabla\tilde{G}=\nabla a$ be our proxy for the group velocity, this is equivalent to requiring that $\tilde{\mathbf{c}}_g\cdot\mathbf{n}>0$.

Continuing, we rewrite (52) as

$$a_{nm}^{(f)}=\frac{ab}{4\pi^2}\int_{-\pi/b}^{\pi/b}\int_{-\pi/a}^{\pi/a}\frac{\mathrm{e}^{\mathrm{i}\mathbf{r}_{nm}\cdot\boldsymbol{\alpha}}}{\tilde{G}(\boldsymbol{\alpha};a,b)}\,\mathrm{d}\boldsymbol{\alpha}, \tag{55}$$

and note that within a stop band $a_{nm}^{(f)}$ may be computed directly from (55) and that the solution decays to zero away from the origin. Outside the stop bands, $\tilde{G}$ vanishes along curves of constant frequency and now the double integral in (55) contains at least one line singularity within the domain of integration. Imposing the radiation condition specifies how the integrals in the inverse Fourier transform (52) should be defined to interpret the effect of this line singularity.

Indeed, the far field wave behaviour is entirely determined by these line singularities and we evaluate their contribution by mapping the integral domain into an orthogonal curvilinear coordinate system which is aligned to each of the curves. The line singularities can then be processed as a continuous integral along each such line. Each integral in the variable perpendicular to the line of singularities can be deformed appropriately around the point where it crosses the singular line, which we assume is now a simple pole, according to its effect on wave radiation at infinity.

Assuming that there are N_c such curves, labelled C_j, $j=1,\ldots,N_c$, along which $\tilde{G}=0$ in the (α,β)-plane for a given fixed frequency a. We parameterise each curve by its arc length s, so that $\boldsymbol{\alpha}=\boldsymbol{\alpha}(s)$ with $|\boldsymbol{\alpha}'(s)|=1$ where the prime denotes differentiation with respect to s. Using the procedure outlined above it follows that, for large $|\mathbf{r}_{nm}|$,

$$a_{nm}^{(f)}\sim\frac{\mathrm{i}ab}{2\pi}\sum_{j=1}^{N_c}\int_{C_j}\frac{\mathrm{e}^{\mathrm{i}\mathbf{r}_{nm}\cdot\boldsymbol{\alpha}(s)}}{\mathbf{n}(s)\cdot\nabla\tilde{G}}\,\mathrm{d}s, \tag{56}$$

where $\mathbf{n}(s)=(\beta'(s),-\alpha'(s))$ denotes the unit normal to the curve C_j. For later convenience, we also define a vector $\hat{\mathbf{n}}(s)=\mu(s)\mathbf{n}(s)$, where $\mu(s)=\pm1$, so that $\hat{\mathbf{n}}$ always points outwards from the origin. In the above, we evaluate the integrals with respect to the coordinate parallel to $\mathbf{n}(s)$ first. If $\hat{\mathbf{n}}\cdot\tilde{\mathbf{c}}_g>0$, the pole represents energy propagating away from the origin, so we deform the contour and complete it in such a way that it encloses the singularity. However, if $\hat{\mathbf{n}}\cdot\tilde{\mathbf{c}}_g<0$, then energy is travelling towards the forced pin, and we deform and complete the integration contour without enclosing the pole. (In this work we have assumed that we are not at a saddle point of the dispersion surface, where $\hat{\mathbf{n}}\cdot\tilde{\mathbf{c}}_g=0$; in such a case the residue would be more complicated than those in Eq. (56). Moreover, the application of the stationary phase

approximation below would need to be adjusted, and would require the use of Airy functions: see the treatment of caustics in Section 4.11 of Lighthill [35].)

The next step in determining the dominant contribution as $|\mathbf{r}_{nm}|\to\infty$ is to identify stationary phase points in the oscillatory integral. These occur at P_j points on the curve C_j given by $s=s_{jk}$ when

$$\mathbf{r}_{nm}\cdot\boldsymbol{\alpha}'(s_{jk})=0,\quad k=1,\ldots,P_j. \tag{57}$$

That is, stationary points are those points on the curve $\tilde{G}=0$ where the radial vector to the point $\mathbf{r}_{nm}$ is perpendicular to that curve, implying $\mathbf{r}_{nm}=|\mathbf{r}_{nm}|\hat{\mathbf{n}}(s)$. Applying the standard result for the method of stationary phase gives

$$a_{nm}^{(f)}\sim\frac{\mathrm{i}ab}{\sqrt{2\pi}}\sum_{j=1}^{N_c}\sum_{k=1}^{P_j}\left.\frac{\mathrm{e}^{\mathrm{i}\mathbf{r}_{nm}\cdot\boldsymbol{\alpha}(s)}\mathrm{e}^{\mathrm{i}\ \mathrm{sgn}(\gamma(s))\pi/4}}{|\gamma(s)|^{1/2}\mathbf{n}(s)\cdot\nabla\tilde{G}}\right|_{s=s_{jk}}, \tag{58}$$

where $\gamma(s)=\mathbf{r}_{nm}\cdot\boldsymbol{\alpha}''(s)=|\mathbf{r}_{nm}|\kappa(s)$, and $\kappa(s)=\mu(s)(\beta'(s)\alpha''(s)-\alpha'(s)\beta''(s))$ is the curvature. Hence we may write (58) as

$$a_{nm}^{(f)}\sim\frac{\mathrm{i}ab}{\sqrt{2\pi|\mathbf{r}_{nm}|}}\sum_{j=1}^{N_c}\sum_{k=1}^{P_j}\left.\frac{\mathrm{e}^{\mathrm{i}\mathbf{r}_{nm}\cdot\boldsymbol{\alpha}(s)}\mathrm{e}^{\mathrm{i}\ \mathrm{sgn}(\kappa(s))\pi/4}}{|\kappa(s)|^{1/2}\mathbf{n}(s)\cdot\nabla\tilde{G}}\right|_{s=s_{jk}}. \tag{59}$$

Note that if there are no stationary points then the summation above equates to zero since we are not attempting to characterise any behaviour in the far-field which decays more rapidly than $|\mathbf{r}_{nm}|^{-1/2}$. Consequently, we have not reconstructed the wave field at infinity, but merely provided an argument for directions of wave radiation and the asymptotic form for the coefficients $a_{nm}^{(f)}$ at infinity in directions where wave radiation is permitted. Specifically, radiation is possible in those directions that cross a dispersion curve parallel to the group velocity vector at the crossing point, and where the group velocity vector also points away from the forced pin.

3.2. Homogeneous defect problem

We now consider the possibility of finding trapped modes, or localised wave motions, due to multiple defects in a doubly periodic lattice of pinned points. A general solution can be written as

$$u^{(d)}(x,y)=\sum_{n=-\infty}^{\infty}\sum_{m=-\infty}^{\infty}a_{nm}^{(d)}g(x-na,y-mb), \tag{60}$$

and we specify $a_{nm}^{(d)}=0$ for $(n,m)\in\mathcal{M}$ which represents that there is no contribution to the displacement from the set $\mathcal{M}$ of pins that have been removed from the lattice. This is a homogeneous problem with no forcing, and we seek nontrivial coefficients $a_{nm}^{(d)}$ for $(n,m)\notin\mathcal{M}$ satisfying the pin conditions $u^{(d)}(pa,qb)=0$ for $(p,q)\notin\mathcal{M}$. Letting $u_{pq}^{(d)}=u^{(d)}(pa,qb)$ represent the unknown plate displacements for $(p,q)\in\mathcal{M}$ we can write

$$u^{(d)}(x,y)=\sum_{(p,q)\in\mathcal{M}}u_{pq}^{(d)}u^{(f)}(x-pa,y-qb). \tag{61}$$

Thus, we can see that $u^{(d)}(pa,qb)=0$ if $(p,q)\notin\mathcal{M}$, and that

$$a_{nm}^{(d)}=\sum_{(p,q)\in\mathcal{M}}u_{pq}^{(d)}a_{n-p,m-q}^{(f)}, \tag{62}$$

so if $(n,m)\in\mathcal{M}$

$$0=\sum_{(p,q)\in\mathcal{M}}u_{pq}^{(d)}a_{n-p,m-q}^{(f)}. \tag{63}$$

Thus, we have a homogeneous system for the unknown displacements $u_{pq}^{(d)}$ at the defects. In other words, the determinant of the matrix

$$\mathbf{K}_{nmpq}=a_{n-p,m-q}^{(f)},\quad (n,m),(p,q)\in\mathcal{M}, \tag{64}$$

is required to vanish for trapping solutions to exist (since we require that $u_{pq}^{(d)}$ for $(p,q)\in\mathcal{M}$ are not all zero). The Toeplitz matrix $\mathbf{K}$ is sized $N\times N$, where N represents the number of defect points contained in the set $\mathcal{M}$. Computing the kernel of $\mathbf{K}$ allows us to calculate the corresponding trapped mode(s) from (61). If the kernel of $\mathbf{K}$ were empty, the $u_{pq}^{(d)}$ would all be zero, and the lattice may as well have been pinned periodically with no defects. Then we would return to the Bloch–Floquet problem discussed earlier where trapping solutions cannot exist.

To compute the shape of the trapped modes inside the defect we need to compute the nonzero $u_{pq}^{(d)}$ given in (63). This is done by first determining the kernel of the Toeplitz matrix $\mathbf{K}$ from which we can then compute the scattering coefficients in (62) allowing us to construct the displacement (60) after suitable truncation of both sums. In practice this can be done by finding the eigenvector(s) of $\mathbf{K}$ with eigenvalue zero.

Since G is real, if we work at frequencies a that lie in a stop band (so that G does not vanish in the domain integral of (52)) then we are assured that $a_{nm}^{(f)}$ is real and hence the determinant of $\mathbf{K}_{nmpq}$ is also real. Thus, the task of finding trapping solutions is simply one of finding real frequencies that force a real determinant to vanish. We note that the realness and

symmetry of $\mathbf{K}_{nmpq}$ implies that the number of linearly independent trapped modes is equal to the multiplicity of the zero eigenvalue.

It is instructive to consider the case where there is only a single defect at the origin, so that $\mathcal{M}=\{(0,0)\}$ and then from (62) the requirement for a trapped mode (52) is simply

$$0=a_{00}^{(f)}=\frac{1}{4\pi^2}\int_0^{\pi}\int_0^{\pi}\frac{1}{G(\theta,\phi;a,b)}\,\mathrm{d}\theta\,\mathrm{d}\phi. \tag{65}$$

Clearly, for solutions of (65) to exist, we require G^{-1} to take different signs in the domain $0<\theta,\phi<\pi$. Since $\lambda(t_0)=-\mathrm{i}(1-\theta^2)^{1/2}$ where $t_0\in(0,1)$ we see immediately that $G^{-1}(\theta,\phi;a,b)=0$ along the circle $\theta^2+\phi^2=1$. This provides a good motivation for seeking a trapped mode solution. For larger values of a, where $|t_n|<1$ for values of n other than zero, G^{-1} also vanishes along curves $\phi^2+(\theta+2n\pi/a)^2=1$, but such arguments are redundant as numerical results would suggest that such values of a lie outside a stop band.

3.3. Lines of defects: Fabry–Perot resonances

Assume now that entire rows are left unpinned in an otherwise doubly periodic array of pinned points. For such a configuration we seek solutions which are trapped by the lines of defects and rapidly decay away from the defect lines. Such solutions are often referred to as Fabry–Perot resonances, or waveguide modes. The missing pins are assumed to lie along the rows $y=mb$ where $m\in\mathcal{M}\subset\mathbb{Z}$. In the simplest case where a single line of pins are removed along $y=0$, $\mathcal{M}=\{0\}$. The general solution can be written as in (60) with $a_{nm}^{(d)}=0$ for $n\in\mathbb{Z}$ and $m\in\mathcal{M}$. Clearly there is no periodicity in the y-direction of the array, however it remains periodic in the x-direction. Consequently any solution must be quasi-periodic in x; that is, they must satisfy

$$u^{(d)}(x+pa,y)=u^{(d)}(x,y)\mathrm{e}^{\mathrm{i}p\theta}, \tag{66}$$

where unlike in previous sections, θ is a freely chosen parameter which reflects the quasi-periodicity of the solution whilst $p\in\mathbb{Z}$. Consequently $a_{nm}^{(d)}=a_{0m}^{(d)}\mathrm{e}^{\mathrm{i}n\theta}$ (which can be shown by examining (66) in terms of (60)) and therefore (60) becomes

$$u^{(d)}(x,y)=\sum_{m=-\infty}^{\infty}a_{0m}^{(d)}\sum_{n=-\infty}^{\infty}\mathrm{e}^{\mathrm{i}n\theta}g(x-na,y-mb). \tag{67}$$

We then apply the pinned conditions $u_{0q}^{(d)}\equiv u^{(d)}(0,qb)=0$ for $q\notin\mathcal{M}$, which only has to be made along $x=0$, since all other values of x have been accounted for by (66). This gives

$$\sum_{m=-\infty}^{\infty}a_{0m}^{(d)}\sum_{n=-\infty}^{\infty}\mathrm{e}^{-\mathrm{i}n\theta}g(na,(q-m)b)=\sum_{r\in\mathcal{M}}u_{0r}^{(d)}\delta_{qr}\quad\forall q\in\mathbb{Z}, \tag{68}$$

where the $u_{0,q}^{(d)}$ $(q\in\mathcal{M})$ are the unknown plate displacements along $(x,y)=(0,qb)$ (i.e. along the cross-section $x=0$ perpendicular to the line of defects). Multiplying (68) by $\mathrm{e}^{-\mathrm{i}q\phi}$ and summing over all q transforms (68) into

$$A^{(d)}(\phi)G(\theta,\phi;a,b)=\sum_{q\in\mathcal{M}}u_{0q}^{(d)}\mathrm{e}^{-\mathrm{i}q\phi}, \tag{69}$$

where we now have

$$A^{(d)}(\phi)=\sum_{m=-\infty}^{\infty}a_{0m}^{(d)}\mathrm{e}^{-\mathrm{i}m\phi}, \tag{70}$$

and G is the double-lattice sum for the infinite periodic array defined as in (46). The θ-dependence is implicit in $A^{(d)}$ and $u_{0q}^{(d)}$.

Rearranging (69) for $A^{(d)}(\phi)$, inverting the transform defined in (70) to return to $a_{0m}^{(d)}$, and then applying the conditions $a_{0m}^{(d)}=0$ for $m\in\mathcal{M}$ gives the homogeneous system of equations

$$0=\sum_{q\in\mathcal{M}}u_{0q}^{(d)}\int_{-\pi}^{\pi}\frac{\mathrm{e}^{\mathrm{i}(m-q)\phi}}{G(\theta,\phi;a,b)}\,\mathrm{d}\phi,\quad m\in\mathcal{M}. \tag{71}$$

Thus, for a Fabry–Perot resonance or trapped mode, we require the determinant of the Toeplitz matrix

$$\mathbf{K}_{mq}^{(d)}=\int_0^{\pi}\frac{\cos((m-q)\phi)}{G(\theta,\phi;a,b)}\,\mathrm{d}\phi,\quad m,q\in\mathcal{M}, \tag{72}$$

to vanish. We note again that G is real, so provided it is also nonzero for $0<\phi<\pi$ for a given value of θ, the integral (72) is real and the determinant of the matrix defined by (72) is also real.

4. Results and discussion

4.1. Forcing and scattering in one dimensional arrays

We begin by considering the one dimensional array problem of a forced pin (a defect subject to time harmonic forcing of unit amplitude), which is shown for an array of period $a=2\pi$ in Fig. 1(a). In this figure we can see clear left–right and up–down symmetry in the computed field, as well as clear energy radiation as we move away from the forcing location at the origin. As outlined in Section 2.2, we show that it is possible to express the unknown coefficients for the scattering problem in terms of the coefficients for the forcing problem. This leads us to Fig. 1(b), where the total field is computed for a particular scattering problem. A plane wave is normally incident on the array from $y>0$, so that $\theta_0=0$ with $a=\pi$. In this configuration no other diffraction orders are excited, and so we can determine the reflection and transmission coefficients straightforwardly as $R=|R_0|^2=0.67801$ and $T=|T_0|^2=0.32199$.

Thus, the symmetry of the plate displacement about the line of pins shown in Fig. 1(b) is due to it being a particular snapshot in time of the superposition of a totally transmitted plane wave and a symmetric circular outgoing wave from the defect. Vertical channels of minimal displacement can be observed both above and below this single defect. We also observe a focusing of energy at the origin where the pin has been removed.

For a plane wave with incident angle $\theta_0=\pi/6$, Fig. 2(a) shows a snapshot in time of a different scattered wave pattern. There is again a defect at the origin. In this plot we can clearly see the formation of partial standing waves above the grating, caused by a large amount of reflection of wave energy by the array (as previously, no other diffraction orders are excited and so $R=|R_0|^2=0.87550$ and $T=|T_0|^2=0.12449$). However, below the grating we can see the interaction effect

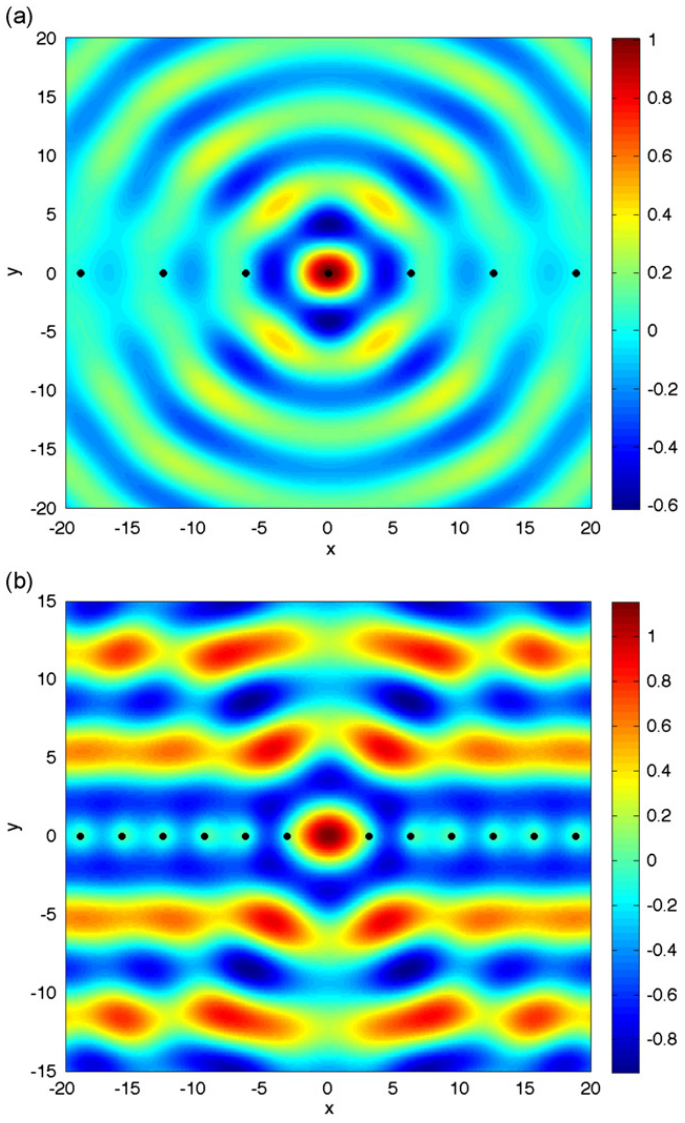

Fig. 1. (a) Total field ($\mathrm{Re}\{u^{(f)}\}$) for a single array of period $a=2\pi$ with a single defect at $\mathcal{M}=\{0\}$ when the central pin is forced. (b) Total field ($\mathrm{Re}\{u^{(s)}\}$) demonstrating scattering by a plane wave at normal incidence on a defective array with $a=\pi$, $\mathcal{M}=\{0\}$.

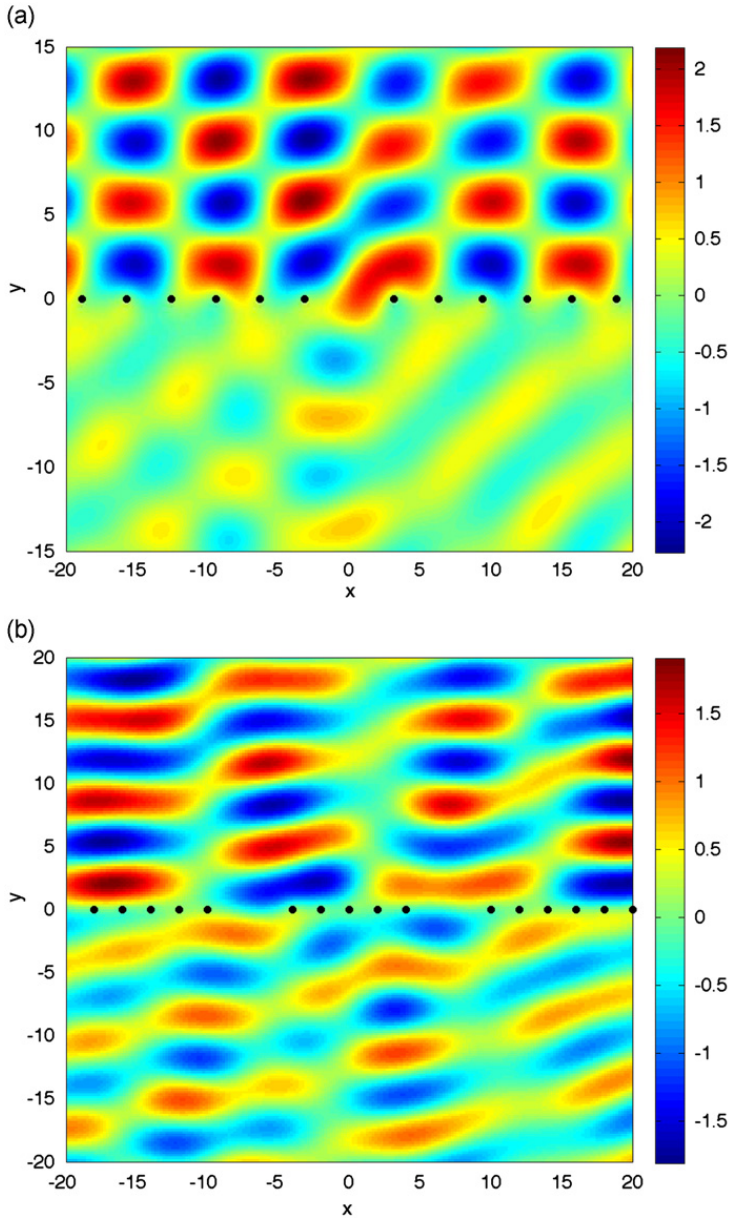

Fig. 2. (a) Total field (Re$\{u^{(s)}\}$) demonstrating scattering by a plane wave at angle $\theta_i = \pi/6$ on a defective grating with $a = \pi$ and $\mathcal{M} = \{0\}$. (b) Total field (Re$\{u^{(s)}\}$) demonstrating scattering by a plane wave at angle $\theta_i = \pi/12$ incident on a single array of period $a=2$ with a four defects at index locations $\mathcal{M} = \{-4,-3,3,4\}$.

between the transmitted wave energy and circular waves emanating from the defect, with occasional destructive interference being produced to the left of the defect.

Using our formulation we can also consider the effects of multiple pins being removed, as shown in Fig. 2(b) where for a single array of period $a=2$, four defects have been removed to recreate a double-slit experiment. For this problem we consider an incident wave at $\theta_0 = \pi/12$, which corresponds to a higher level of energy transmission ($R = |R_0|^2 = 0.57652$ and $T = |T_0|^2 = 0.42348$). Here the circular waves emanating from the defects also have a strong effect, with a clear channel of minimal displacement directed downwards and to the right from the right hand defect.

4.2. Forcing and band surfaces for doubly periodic arrays

We now consider the problem of determining the band surfaces of our pinned plate, which allows us to determine information about the propagating modes, or Bloch modes, that are supported by our doubly periodic medium [36]. From this, the band surfaces also reveal the locations of full orpartial stop bands, which correspond to frequencies at which no propagation through the array is possible, for given (θ,ϕ) values. It is in these stop bands that we look for trapping behaviour when defects are introduced.

Movchan et al. [13] considered the particular case of a square array of pins ($b/a=1$) by taking limits of a more general system based on multipole expansions designed to investigate the band-gap structure of periodic arrays of finite-radius circular holes. Thus, when the radius of a clamped hole tended to zero, a simplified dispersion relation was derived in terms of lattice sums for the Helmholtz and modified Helmholtz equations (see Eq. (6.2) of [13]). As outlined in their paper and in [32], the computation of these lattice sums is extremely complicated. Here, we have derived an alternative dispersion relation (53) in which the lattice sum (50) is both convergent and simple to compute. Our solutions coincide with those in Movchan et al. [13], who were also able to determine that the band surfaces for arrays of pins were bound between singularities arising from these lattice sums. These singularity curves correspond to discrete values at which

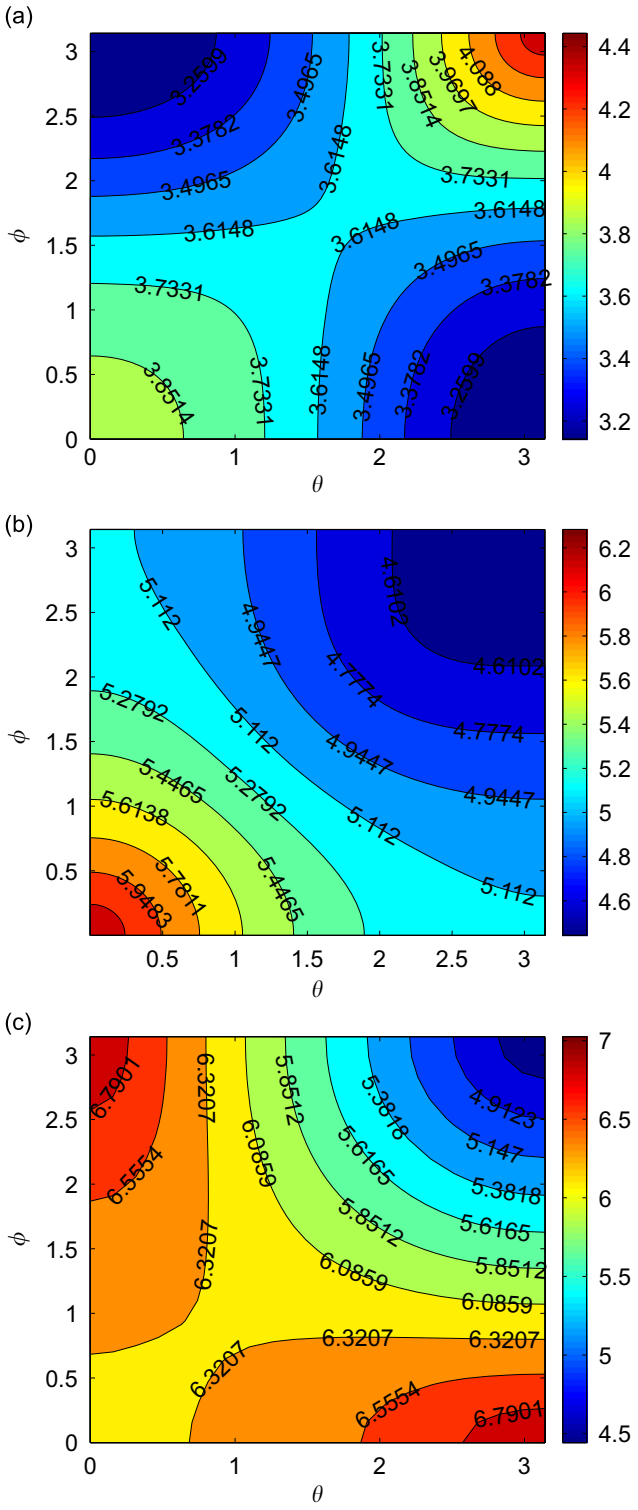

Fig. 3. (a) Contour plot of a values constituting the first band surface, over 1/4 of the Brillouin zone, for a doubly periodic square array of pinned points $b/a=1$. Figs. (b) and (c) show the second and third band surfaces (respectively) over 1/4 of the Brillouin zone.

plane wave solutions would be supported in the medium in the absence of our pins [39]. This acts as a useful tool for computing solutions of (53) as an upper and lower bound for each zero can be determined straightforwardly.

To determine the band surfaces from (53) we search for values of a (which is a dimensionless proxy for the wavenumber) for given values of θ and ϕ (which are themselves proxies for Bloch vector elements). For the case of a square array ($b/a=1$) we show the first, second and third band surfaces in Fig. 3(a)–(c) (respectively) over a quarter of the Brillouin zone. A full picture of the band surface over the entire Brillouin zone can be obtained by reflection in the θ and ϕ axes. From the picture of the first band surface we can deduce that we have a complete stop band from $0<a<\pi$, and by comparing Fig. 3(a) and (b), that only partial stop bands exist between the first and second band surfaces (i.e. the stop band frequency depends on θ and ϕ). Movchan et al. [13] show that only partial stop bands exist between all other higher order band surfaces. Additionally, we note that the width of the first stop band is proportional to the spacing ratio b/a, that is, the first stop band exists in the range $0<a<\pi/(b/a)$ for rectangular arrays, as outlined in Section 3.1.

In Section 3.1 it was shown that wave radiation through the array from a forced pin can only occur when the Bloch vector $\boldsymbol{\alpha}$ and the vector tangent to a constant frequency curve on the dispersion surface are at right angles, and provided the gradient $\nabla a=\tilde{\mathbf{c}}_g$ of the dispersion surface also points away from the origin at any such points. Thus, the amplitude of the wave radiated to infinity is inversely proportional to both the magnitude of that gradient and to the square root of the curvature along a curve of constant frequency.

Now, since $b/a=1$, directions in $\boldsymbol{\alpha}$-space are the same as in (θ,ϕ)-space. Moreover, if wave propagation is possible in a certain direction of $\boldsymbol{\alpha}$-space, then it is also possible in the same direction of (x,y)-space. Thus, observing Fig. 3(a) and (b) we can say the following. For $0<a<\pi$ there is no wave radiation to infinity as the frequency lies in a stop band. Then, as a increases from π to approximately 3.6238 (the level of the saddle point) there is still no wave radiation as the only possible directions for wave propagation are along $x=0$ and $y=0$, but there the gradient of the dispersion surface along outgoing lines is negative. As a increases beyond 3.6238, again the lines $x=0$ and $y=0$ are excluded from wave radiation as the gradient is negative but wave radiation along $x=y$ (and by reflection along $x=-y$) is allowed, determined by values of θ and ϕ in the portion of the dispersion surface for which the gradient is positive. The amplitude factor of radiated waves is large for a close to the value at the saddle point where the gradient is close to zero (here the group velocity is small and so energy only propagates slowly away from the origin) and decreases as a increases up to the point at which we switch from the first band to the second band ($a\simeq 4.4429$). According to the second band, all possible directions of wave radiation are associated with negative gradients on the dispersion surface and therefore there is no wave radiation to infinity associated with this band. However, moving on to Fig. 3(c), we can see that the third band also starts at $a\simeq 4.4429$ and in this case there are possible directions of wave radiation to infinity along $x=0$ and $y=0$ for values between $a\simeq 6.3137$ and $a\simeq 7.0248$ where the gradients of the dispersion surfaces are increasing.

The overall picture is one in which the scope to radiate waves from an oscillating source at the origin to infinity is limited, even if the frequency is inside a band surface. However, we have shown that oscillations within certain higher frequency ranges can send waves through the lattice in different directions (here either along $x=y$ for $3.6238<a<4.4429$ or along the axes if $6.3137<a<7.0248$).

In Fig. 4 we show a snapshot in time of the plate displacement when a central pin in a doubly periodic pinned plate is made to oscillate with unit amplitude at a dimensionless value of $a=1$ and spacing ratio of $b/a=1/2$. This corresponds to a frequency within the stop band for the doubly periodic array ($0<a<2\pi$ when $b/a=1/2$) and hence the figure confirms that there is no energy propagation to infinity. Indeed, the displacement is predominantly contained horizontally within one layer of pins, and contained vertically within two layers.

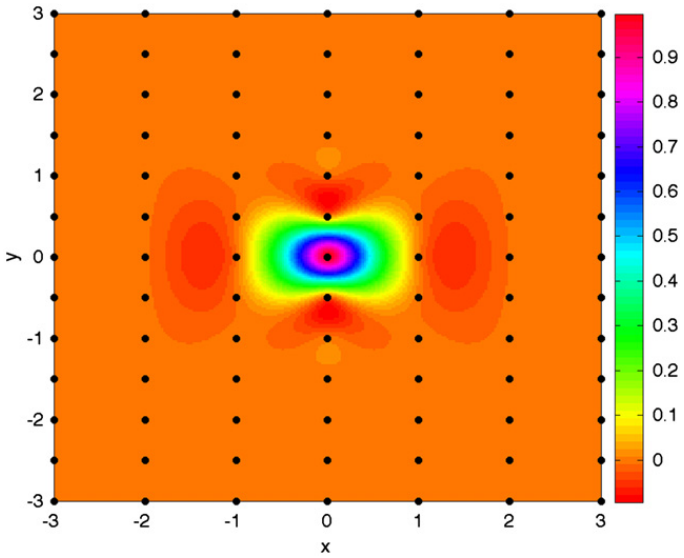

Fig. 4. Total field ($\mathrm{Re}\{u^{(f)}\}$) for the forcing of the central pin $\mathcal{M}=\{0,0\}$ in a doubly periodic array with periodicity $a=1$, $b=1/2$.

4.3. Trapped modes in doubly periodic arrays with defects

We now examine the different mode shapes that can be supported inside defects which exist in doubly periodic square arrays. We look for the resonant frequencies of these defects inside the first stop band, which for square arrays ($b/a=1$) is the interval $0<a<\pi$. Each trapped mode corresponding to a nondegenerate frequency was also confirmed by exciting a large finite cluster, with the same defect in its centre, with an incident wave. At degenerate frequencies, different combinations of the two possible trapped modes appeared, depending on the angle of incidence and the relative closeness of the frequencies. It would be an interesting problem to attempt to predict how the excited modes depend on this angle, but one which is not attempted here.

We begin by determining the resonant frequencies for two problems—firstly, a single defect at the origin, and secondly, a 3×3 sized defect cluster centred about the origin where pins corresponding to the indices $(-1,0,1)\times(-1,0,1)$ are removed. This is done by evaluating the determinant of the Toeplitz matrix $\mathbf{K}_{mnpq}$ as given in (64) for varying a. We can see from Fig. 5(a) that only one resonant frequency exists in the first stop band for the single defect problem and is given by $a\simeq2.53727$. This compares well with the estimate $a\simeq2.538$ given in McPhedran et al. [40] which was evaluated by computing the kernel of a truncated matrix of standard Green's functions (of the form given in (7)).

For the 3×3 defect we can see from Fig. 5(b) that there are resonant frequencies at $a\simeq1.35692$, 1.95271, 2.38206, 2.61818, 2.62461 and $a\simeq2.93110$. In this case we have the added complication of degenerate (repeated) roots corresponding to the determinant curve touching the zero axis as opposed to crossing it completely. These degenerate frequencies are a consequence of the symmetry of the geometry and the associated trapped mode. That is, it is possible for two modes to exist for the same frequency a, one with a line of symmetry in $x=0$ and the other in $y=0$. If $a/b\neq1$ then modes symmetric in x are different to modes symmetric in y, eliminating the presence of repeated roots.

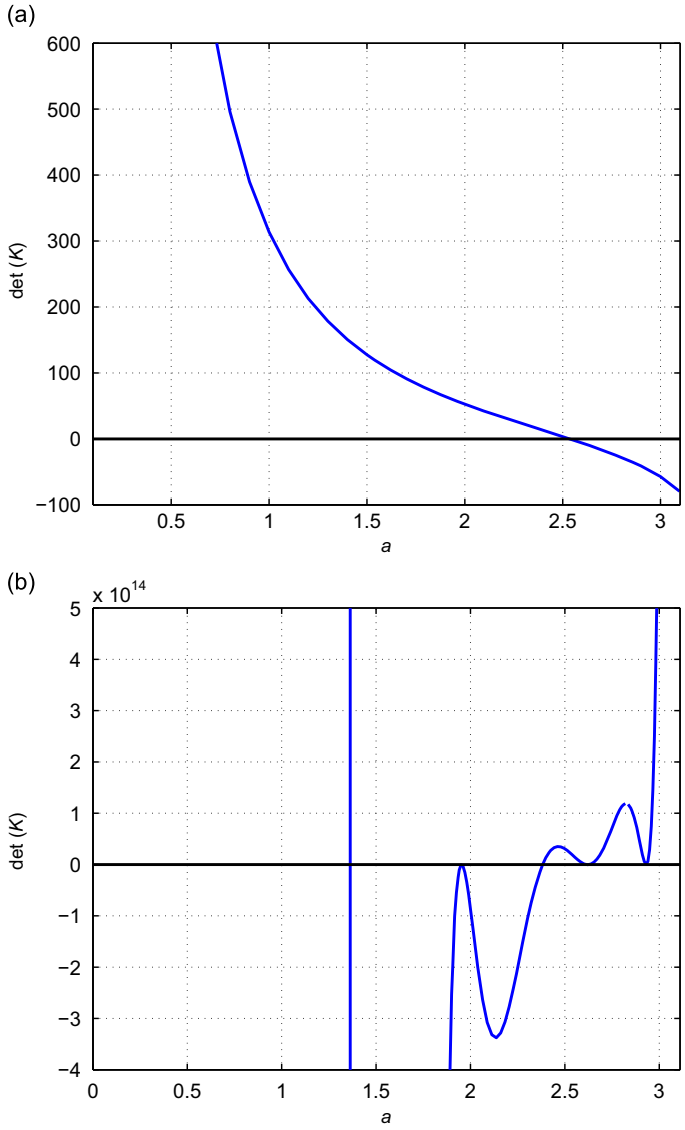

Fig. 5. (a) Determinant of Toeplitz matrix $\mathbf{K}_{m,n,p,q}$ for a single defect at the origin, with a single defect frequency at $a\simeq2.53728$ for $b/a=1$. (b) Determinant of Toeplitz matrix $\mathbf{K}_{m,n,p,q}$ for a 3×3 defect, with multiple defect frequencies.

The discontinuity of the determinant curve in Fig. 5(b) at $a=2.82743$ is associated with the determinant of **K** becoming infinitely large. This is a consequence of the Green's function being undefined at this value of a for all $0<\theta<\pi$ (when $b/a=1$), and does not correspond to a trapped mode.

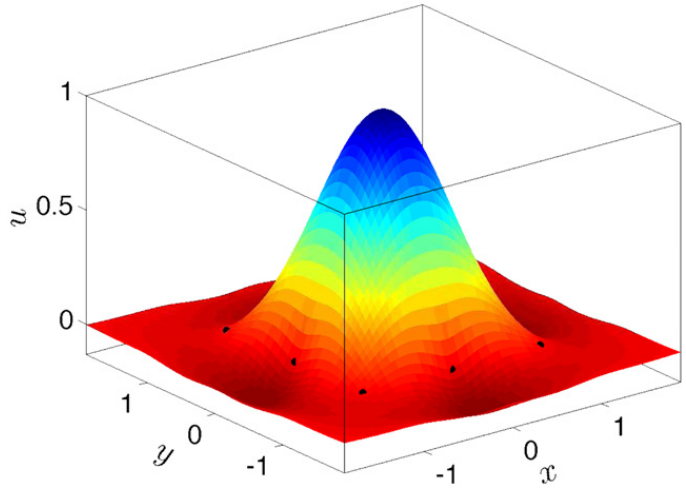

Fig. 6. Mode shape ($\mathrm{Re}\{u^{(d)}\}$) for a single defect in doubly periodic domain $a\simeq 2.53728$, $b/a=1$.

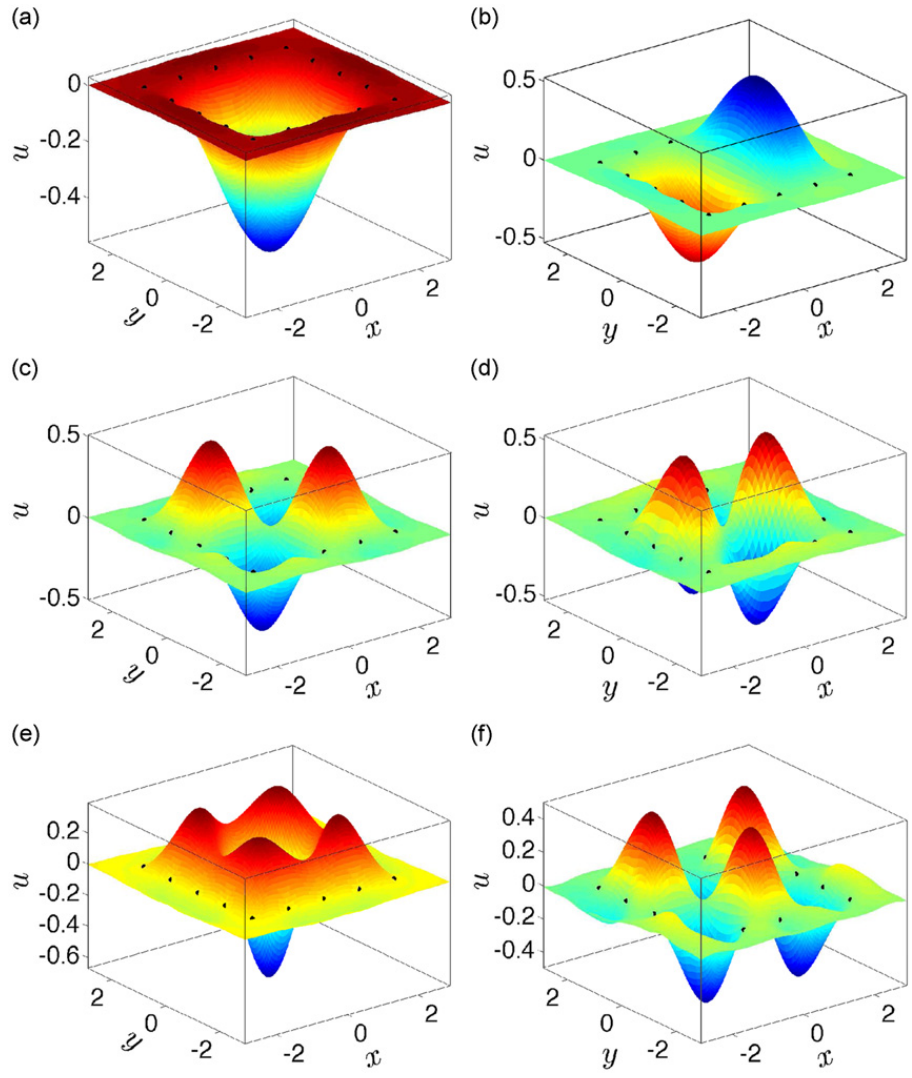

Fig. 7. Mode shapes that are supported inside 3×3 defect in doubly periodic domain ($b/a=1$) at (a) $a\simeq 1.35692$, (b) $a\simeq 1.95271$, (c) $a\simeq 2.38206$, (d) $a\simeq 2.61818$, (e) $a\simeq 2.62461$, and (f) $a\simeq 2.93110$.

Returning to the single defect problem, the mode shape corresponding to $a \simeq 2.53728$ is computed in Fig. 6 which shows one peak, symmetric about both $x=0$ and $y=0$ which is well trapped inside the defect with negligible displacement throughout the surrounding array.

For the 3×3 defect the associated modes are given in Fig. 7. A number of these mode shapes have clear reflection and rotational symmetry inside the defect, most notably those corresponding to the degenerate frequencies which are given in Fig. 7(b), (e), and (f). Some of the mode shapes computed here are reminiscent of the mode shapes for square plates that are completely clamped, as discussed in [41]. Again, we observe a rapid decay of displacement with distance away from the defect into the array in all figures.

We finally consider a 4×1 defect in a square array ($b/a=1$), for which all trapped mode frequencies are distinct (i.e. not repeated roots) in the first stop band. The corresponding mode shapes are given in Fig. 8 and bear resemblance to the first few harmonics for waves on a string, which is not unexpected given the slender geometry of our defect cluster.

4.4. Fabry–Perot line defects in two-dimensional arrays

For the waveguide problem, we remove entire rows of pins from the otherwise perfect doubly periodic array. We then vary our quasi-periodicity parameter θ and look for values of a that satisfy the relation given by (72), which essentially reveals the frequencies at which different waveguide modes are supported inside the defect(s). These waveguide modes transport wave energy inside the line defects without leakage into the surrounding array. There may still be some motion outside the defect but its amplitude rapidly decays with distance away from it.

In Fig. 9(a) we examine (72) for the case of a single line defect ($m=0$) for multiple aspect ratios b/a. We can see that for this single line defect ($b/a=1$) we have a single curve which exists in the interval $1.96720 < a < \pi$. We see similarly sloped curves for $b/a=1.5$ and $b/a=2$, which end abruptly when they approach the edge of their first stop bands (for example, when $b/a=2$, the stop band interval is $0 < a < \pi/2$).

In Fig. 9(b) we consider the case when we have two nonneighbouring line defects ($m=0, -3$) for multiple aspect ratios b/a. For $b/a=1$, (72) reveals two unique values of a over an interval of θ values, which corresponds to one symmetric mode and one antisymmetric mode supported across both line defects (represented by the broken and solid lines, respectively). In a small interval near $\theta \simeq 2.25$ the waveguide mode frequencies a become nearly degenerate but nevertheless two distinct modes always exist. The curves for $b/a=1.5$ and $b/a=2$ are similar, but the near-degeneracy occurs at lower values of a and θ, and there is no clear splitting near the approach to the first stop band when compared to the $b/a=1$ curve.

For the single line defect problem, the waveguide mode corresponding to $b/a=1$, $a=2.1$, $\theta=0.87850$ is computed using (67) and shown in Fig. 10(a). This mode is well contained with only small troughs existing outside the defect when the mode itself is at a minimum. For the doubly periodic problem, the waveguide mode corresponding to $b/a=1$, $a=2.1$, $\theta=0.75567$ is given in Fig. 10(b) and in Fig. 10(c) the mode corresponding to $\theta=0.97115$ is shown. From Fig. 10(b) we can take a vertical slice through the field and determine that this first mode is antisymmetric, and as before, we have some

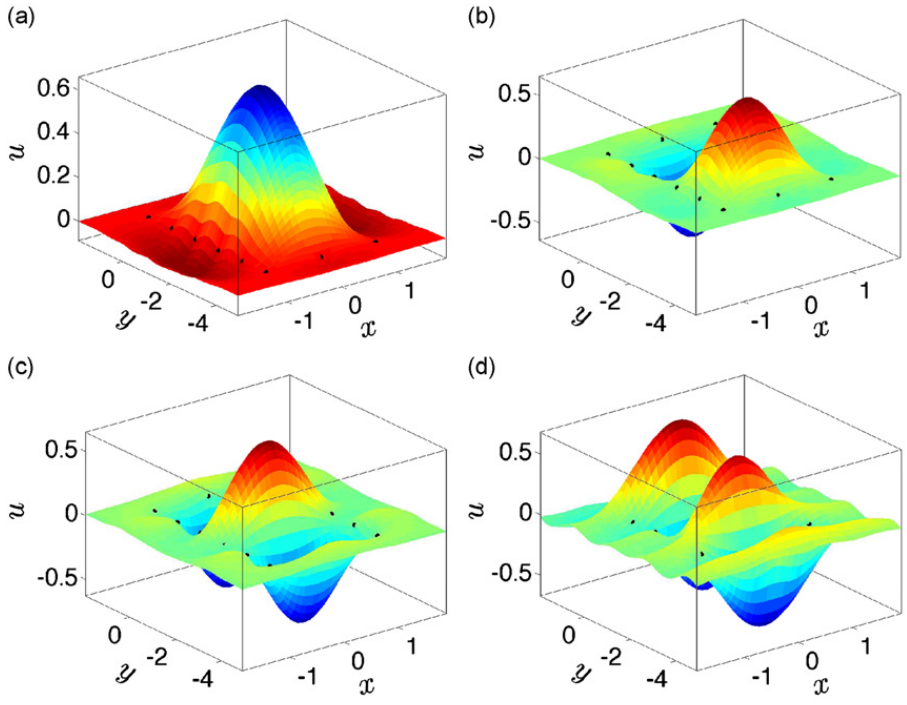

Fig. 8. Mode shapes that are supported inside 4×1 defect (or 1×4 defect) in doubly periodic domain ($b/a=1$) at (a) $a \simeq 2.04864$, (b) $a \simeq 2.28328$, (c) $a \simeq 2.63330$, and (d) $a \simeq 3.03234$.

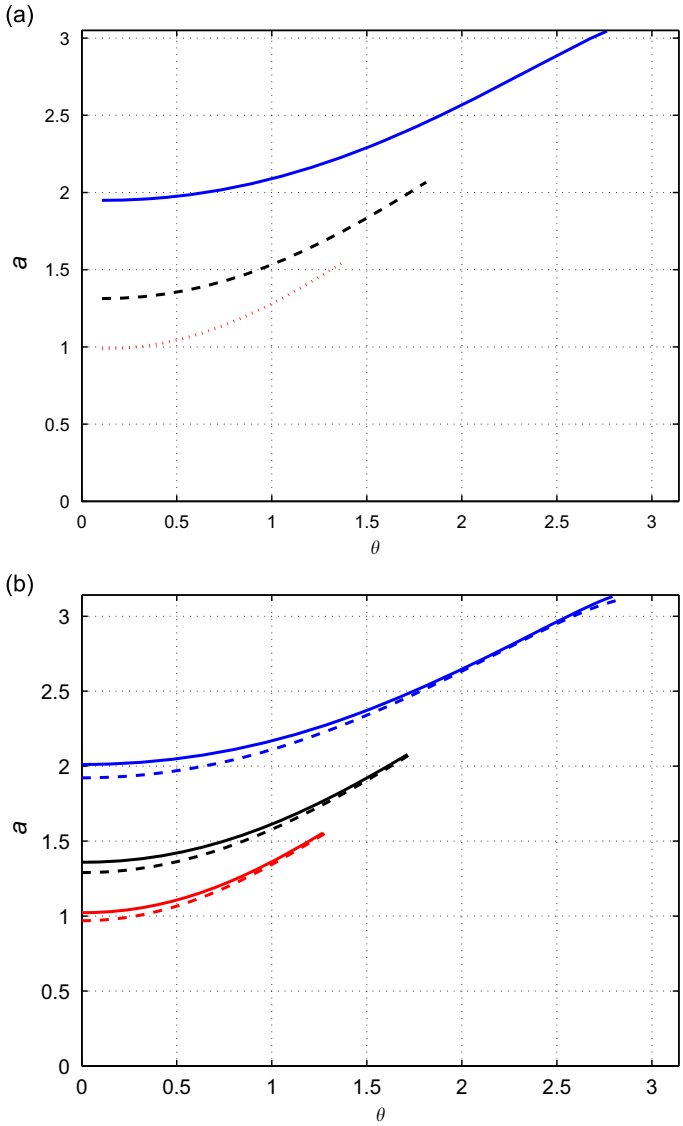

Fig. 9. (a) Plot showing the values of a for which $\det\{\mathbf{K}_{m,q}\}=0$ for a single line defect ($m=0$). (b) Values of a when $\det\{\mathbf{K}_{m,q}\}=0$ for the two line defect case ($m=0, -3$) where $b/a=1$ (blue curve), $b/a=1.5$ (black curve), and $b/a=2$ (red curve). (For interpretation of the references to color in this figure caption, the reader is referred to the web version of this article.)

displacement occurring outside the array corresponding to minima in the mode, with little interaction in the space between the two channels. For Fig. 10(c) we have the second waveguide mode which is symmetric and demonstrates minimal displacement outside the line defects for $x<0$. However, there is now a strong interaction between the two channel defects.

5. Conclusions

In this paper we have examined a number of problems connected with defects in one- and two-dimensional rectangular arrays of periodically pinned plates. A method has been outlined for analytically determining a variety of properties of the solution including the plate displacement for problems where a single pin within the array is forced to oscillate and where incident waves are diffracted by a one-dimensional pinned array in which multiple pins are removed. For two-dimensional arrays, we have also provided analytical expressions to determine certain localised modes which exist when either a finite number of pins are removed or entire rows are removed. Connections between forced pin problems and scattering and trapping problems in which pins are removed have been highlighted in both one- and two-dimensional situations. This has similarities to the work of Thompson and Linton [18] for a related problem in acoustics. The exact description of the infinite array has been included by Fourier transforming infinite systems of equations, thus avoiding the use of supercell methods as in Poulton et al. [25] or by interpreting results from a truncated array approximation.

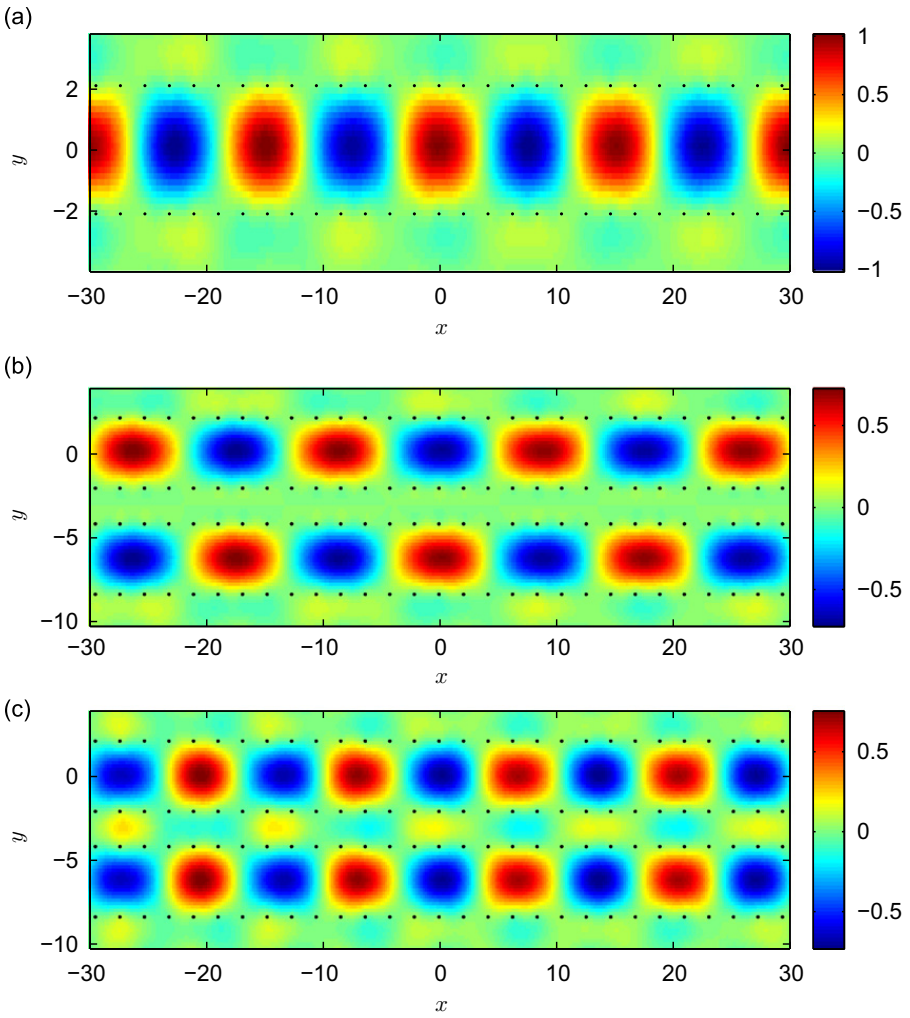

Fig. 10. (a) Waveguide mode ($\mathrm{Re}\{u^{(d)}\}$) for a single line defect at $\theta = 0.87850$ for $a=2.1$, $b/a=1$. (b and c) Waveguide modes for a double line defect corresponding to (b) $\theta = 0.75567$ and (c) $\theta = 0.97115$ with $a=2.1$ and $b/a=1$.

We have also shown theoretically how to determine the discrete directions at which waves may radiate through a doubly periodic array in which the central pin is forced to oscillate and shown that different frequency ranges lead to wave radiation in different directions. In addition, we derived the asymptotic amplitudes of the source strengths in these directions.

There are a number of interesting extensions to the current work that could be made. For example, the problem of plane wave scattering by either one- or two-dimensional semi-infinite periodic arrays of pins could be solved using the discrete Wiener–Hopf technique as done by [42,43] for scattering of long waves by cylinders. Defects (particularly line defects) could also be put introduced into their formulations in a relatively straightforward manner.

Another straightforward extension of the methods presented here can be made for problems involving defects in a semi-infinite elastic plate which is pinned periodically along its free edge. The solution for the corresponding problem without defects has been presented in [44] which simply requires that the Green's function representing the effect of each pin be altered, to take account of the free edge conditions [45].

References

[1] F.G. Leppington, Acoustic scattering by membranes and plates with line constraints, *Journal of Sound and Vibration* 58 (3) (1978) 319–332.
[2] D.G. Crighton, Transmission of energy down periodically ribbed elastic structures under fluid loading, *Proceedings of the Royal Society of London Series A: Mathematical and Physical Sciences* 394 (1807) (1984) 405–436.
[3] M. Spivack, Wave propagation in finite periodically ribbed structures with fluid loading, *Proceedings of the Royal Society of London Series A: Mathematical and Physical Sciences* 435 (1895) (1991) 615–634.
[4] M.B. Sobnack, D.G. Crighton, Effect of an isolated irregularity on the transmission of energy down a periodically ribbed fluid-loaded elastic structure, *Proceedings of the Royal Society of London Series A: Mathematical and Physical Sciences* 441 (1913) (1993) 473–494.
[5] A.J. Cooper, D.G. Crighton, Transmission of energy down periodically ribbed elastic structures under fluid loading: spatialperiodicity in the pass bands, *Proceedings of the Royal Society A: Mathematical, Physical and Engineering Sciences* 454 (1979) (1998) 2893.
[6] M.B. Sobnack, D.G. Crighton, Anderson localization effects in the transmission of energy down an irregularly ribbed fluid-loaded structure, *Proceedings of the Royal Society of London Series A: Mathematical and Physical Sciences* 444 (1920) (1994) 185–200.

[7] D.V. Evans, R. Porter, Penetration of flexural waves through a periodically constrained thin elastic plate in vacuo and floating on water, *Journal of Engineering Mathematics* 58 (1) (2007) 317–337.
[8] D.V. Evans, R. Porter, Wave diffraction by a periodically constrained elastic plate floating on water, *Proceedings of the 21st International Workshop on Water Waves and Floating Bodies*, Loughborough, UK, 2006.
[9] P.A. Martin, *Multiple Scattering: Interaction of Time-harmonic Waves with N Obstacles*, Vol. 107, Cambridge University Press, Cambridge, 2006.
[10] I.V. Andronov, Waves propagating along a periodic set of point inhomogeneities in a thin elastic plate, *Acoustical Physics* 56 (3) (2010) 259–267.
[11] D.P. Kouzov, V.D. Lukyanov, Influence of point inhomogeneities on vibrations of a thin plate, *Mekhanika tverdogo tela* 10 (6) (1975) 117–123.
[12] D.P. Kouzov, V.D. Lukyanov, Acoustic transmittivity of a thin elastic plate reinforced at a discrete set of points, *Soviet Physics Acoustics* 22 (1) (1976) 23–27.
[13] A.B. Movchan, N.V. Movchan, R.C. McPhedran, Bloch–Floquet bending waves in perforated thin plates, *Proceedings of the Royal Society A: Mathematical, Physical and Engineering Sciences* 463 (2086) (2007) 2505–2518.
[14] N.V. Movchan, R.C. McPhedran, A.B. Movchan, C.G. Poulton, Wave scattering by platonic grating stacks, *Proceedings of the Royal Society A: Mathematical, Physical and Engineering Sciences* 465 (2111) (2009) 3383–3400.
[15] S.G. Haslinger, N.V. Movchan, A.B. Movchan, R.C. McPhedran, Transmission, trapping and filtering of waves in periodically constrained elastic plates, *Proceedings of the Royal Society A: Mathematical, Physical and Engineering Science* 468 (2137) (2011) 76–93.
[16] M.H. Meylan, R.C. McPhedran, Fast and slow interaction of elastic waves with platonic clusters, *Proceedings of the Royal Society A: Mathematical, Physical and Engineering Sciences* 467 (2136) (2011) 3509–3529.
[17] W.J. Parnell, P.A. Martin, Multiple scattering of flexural waves by random configurations of inclusions in thin plates, *Wave Motion* 48 (2) (2011) 161–175.
[18] I. Thompson, C.M. Linton, An interaction theory for scattering by defects in arrays, *SIAM Journal on Applied Mathematics* 68 (6) (2008) 1783–1806.
[19] I. Thompson, C.M. Linton, On the excitation of a closely spaced array by a line source, *IMA Journal of Applied Mathematics* 72 (4) (2007) 476–497.
[20] M.M. Sigalas, Elastic wave band gaps and defect states in two-dimensional composites, *Journal of the Acoustical Society of America* 101 (3) (1997) 1256–1261.
[21] A. Khelif, A. Choujaa, B. Djafari-Rouhani, M. Wilm, S. Ballandras, V. Laude, Trapping and guiding of acoustic waves by defect modes in a full-band-gap ultrasonic crystal, *Physical Review B* 68 (21) (2003) 214301.
[22] S. Wilcox, L.C. Botten, R.C. McPhedran, C.G. Poulton, C.M. de Sterke, Modeling of defect modes in photonic crystals using the fictitious source superposition method, *Physical Review E* 71 (5) (2005) 056606.
[23] H. Ammari, F. Santosa, Guided waves in a photonic bandgap structure with a line defect, *SIAM Journal on Applied Mathematics* (2004) 2018–2033.
[24] S. Mahmoodian, R.C. McPhedran, C.M. de Sterke, K.B. Dossou, C.G. Poulton, L.C. Botten, Single and coupled degenerate defect modes in two-dimensional photonic crystal band gaps, *Physical Review A* 79 (1) (2009) 013814.
[25] C.G. Poulton, R.C. McPhedran, N.A. Nicorovici, L.C. Botten, Localized Greens functions for a two-dimensional periodic material, in: *IUTAM Symposium on Asymptotics, Singularities and Homogenisation in Problems of Mechanics*, Springer, 2004, pp. 181–190.
[26] A. Figotin, V. Goren, Resolvent method for computations of localized defect modes of H-polarization in two-dimensional photonic crystals, *Physical Review E* 64 (5) (2001) 056623.
[27] D.J. Kan, A.A. Asatryan, C.G. Poulton, L.C. Botten, Multipole method for modeling linear defects in photonic woodpiles, *Journal of the Optical Society of America B* 27 (2) (2010) 246–258.
[28] C.G. Poulton, A.B. Movchan, N.V. Movchan, R.C. McPhedran, Analytic theory of defects in periodically structured elastic plates, *Proceedings of the Royal Society A: Mathematical, Physical and Engineering Science* Vol. 468 (2140), The Royal Society, 2012, pp. 1196–1216. 〈http://rspa.royalsocietypublishing.org/content/468/2140/1196.short〉, http://dx.doi.org/10.1098/rspa.2011.0609.
[29] S.K. Chin, N.A. Nicorovici, R.C. McPhedran, Green's function and lattice sums for electromagnetic scattering by a square array of cylinders, *Physical Review E* 49 (1994) 4590–4602.
[30] C.G. Poulton, L.C. Botten, R.C. McPhedran, A.B. Movchan, Source-neutral Green's functions for periodic problems in electrostatics, and their equivalents in electromagnetism, *Proceedings of the Royal Society A: Mathematical, Physical and Engineering Sciences* 455 (1983) (1999) 1107–1123.
[31] A.B. Movchan, N.V. Movchan, C.G. Poulton, *Asymptotic Models of Fields in Dilute and Densely Packed Composites*, Imperial College Press, London, 2002.
[32] C.M. Linton, Lattice sums for the Helmholtz equation, *SIAM Review* 52 (4) (2010) 630–674.
[33] G.N. Watson, *A Treatise on the Theory of Bessel Functions*, Cambridge University Press, Cambridge, 1995.
[34] P.A. Martin, Discrete scattering theory: Greens function for a square lattice, *Wave Motion* 43 (7) (2006) 619–629.
[35] J. Lighthill, *Waves in Fluids*, Cambridge University Press, Cambridge, 1978.
[36] J.D. Joannopoulos, *Photonic Crystals: Molding the Flow of Light*, Princeton University Press, Princeton, 2008.
[37] P.A. Martin, S.G. Llewellyn Smith, Generation of internal gravity waves by an oscillating horizontal disc, *Proceedings of the Royal Society A: Mathematical, Physical and Engineering Sciences* 467 (2011) 3406–3423, http://dx.doi.org/10.1098/rspa.2011.0193.
[38] P.A. Martin, S.G. Llewellyn Smith, Internal gravity waves, boundary integral equations and radiation conditions, *Wave Motion* 49 (2012) 427–444.
[39] S. Guo, P. McIver, Propagation of elastic waves through a lattice of cylindrical cavities, *Proceedings of the Royal Society A: Mathematical, Physical and Engineering Sciences* 467 (2134) (2011) 2962–2982.
[40] R.C. McPhedran, A.B. Movchan, N.V. Movchan, Platonic crystals: Bloch bands, neutrality and defects, *Mechanics of Materials* 41 (4) (2009) 356–363.
[41] A.W. Leissa, *Vibration of Plates*, NASA SP-160, Washington, DC, 1969.
[42] C.M. Linton, P.A. Martin, Semi-infinite arrays of isotropic point scatterers. A unified approach, *SIAM Journal on Applied Mathematics* 64 (2004) 1035–1056.
[43] N. Tymis, I. Thompson, Low-frequency scattering by a semi-infinite lattice of cylinders, *The Quarterly Journal of Mechanics and Applied Mathematics* 64 (2) (2011) 171–195.
[44] D.V. Evans, R. Porter, Flexural waves on a pinned semi-infinite thin elastic plate, *Wave Motion* 45 (6) (2008) 745–757.
[45] R. Gunda, S.M. Vijayakar, R. Singh, J.E. Farstad, Harmonic Greens functions of a semi-infinite plate with clamped or free edges, *The Journal of the Acoustical Society of America* 103 (1998) 888–899.